Building and Environment 223 (2022) 109489

Contents lists available at ScienceDirect

Building and Environment

journal homepage: www.elsevier.com/locate/buildenv

Controlling infectious airborne particle dispersion during surgical procedures: Why mobile air supply units matter?

Huiyi Tan [a], Keng Yinn Wong [b,c,*], Mohd Hafiz Dzarfan Othman [d], Hong Yee Kek [b], Wah Yen Tey [e], Bemgba Bevan Nyakuma [f], Guo Ren Mong [g], Garry Kuan [h,i], Wai Shin Ho [a,c], Hooi Siang Kang [b], Desmond Daniel Chin Vui Sheng [b], Roswanira Abdul Wahab [d,j]

[a] School of Chemical and Energy Engineering, Faculty of Engineering, Universiti Teknologi Malaysia, Johor, Malaysia
[b] School of Mechanical Engineering, Faculty of Engineering, Universiti Teknologi Malaysia, Johor, Malaysia
[c] Process Systems Engineering Centre, Faculty of Engineering, Universiti Teknologi Malaysia, Johor, Malaysia
[d] Advanced Membrane Technology Research Centre (AMTEC), Universiti Teknologi Malaysia, Johor, Malaysia
[e] Faculty of Engineering, Technology and Built Environment, USCI University, Kuala Lumpur, Malaysia
[f] Department of Chemistry, Faculty of Sciences, Benue State University, Makurdi, Benue State, Nigeria
[g] School of Energy and Chemical Engineering, Xiamen University Malaysia, Sepang, Selangor, Malaysia
[h] School of Health Science, Universiti Sains Malaysia, Kelantan, Malaysia
[i] Department of Life Sciences, Brunel University, Uxbridge, London, United Kingdom
[j] Department of Chemistry, Faculty of Sciences, Universiti Teknologi Malaysia, Skudai, Johor, Malaysia

ARTICLE INFO

Keywords:
Operating room (OR)
Computational fluid dynamic (CFD)
Mobile air supply (MAS)
Particle distribution
Ventilation strategy

ABSTRACT

The ventilation system in an operating room (OR) plays a vital role in reducing the risk of patients contracting an infection while undergoing a surgical procedure. The clean air supplied from the ceiling-mounted diffuser removes the airborne particles from the surgical site. The clean air, however, is often obstructed by the medical staff and other objects. Hence, some sterile instruments might remain outside the protected area. The present study aims to examine the effectiveness of a mobile air supply (MAS) unit in reducing the particle settlement on a patient under different airflow velocities supplied from the MAS unit. A simplified computational fluid dynamics (CFD) model of the OR was developed and validated based on published data. An RNG k-epsilon turbulence model, based on the Reynolds-Averaged Navier-Stokes (RANS) equations, was used to simulate the airflow, while a discrete phase model (DPM) was used to simulate the movement of the infectious airborne particles. The MAS unit was evaluated as an extension of unidirectional airflow ventilation. Results showed that the MAS unit successfully reduced the settlement of airborne particles by 78% from 45 particles/m^3 to 10 particles/m^3. However, the operation of the MAS unit showed a reverse effect on the particle settlement (~7 particles/m^3) on the patient when the MAS unit supplied air at a velocity of 0.6 m/s. The present study showed that air supply at a velocity of 0.5 m/s provided an optimum wiping effect that removed the airborne particles from the surgical zone.

1. Introduction

Health care institutions such as hospitals provide specialized medical-related treatment and nursing care to patients. An operating room (OR) is a facility within a hospital with an aseptic environment, where a team of medical staff members perform surgical procedures on the patients. The indoor environmental conditions in an OR are designed to satisfy the hygiene requirements and needs of patients [1]. The ASHRAE Standard 170–2013 suggests that the air temperature in an OR should be between 20 °C and 24 °C, while the relative humidity should range from 30% to 60% [2]. The relative humidity in the OR varies inversely with the air temperature [3,4]. Typically, an increase in air temperature decreases relative humidity, which also lowers the air moisture. To sustain the OR environment at an ideal level, both relative humidity and air temperature are equally significant and must be considered. Low relative humidity levels reduce the service life of particular supplies such as chemical and biological gauges for monitoring the sterilization process and electrocardiogram electrodes [5,6].

* Corresponding author. School of Mechanical Engineering, Faculty of Engineering, Universiti Teknologi Malaysia, Johor, Malaysia.
E-mail address: kengyinnwong@utm.my (K.Y. Wong).

https://doi.org/10.1016/j.buildenv.2022.109489
Received 10 May 2022; Received in revised form 22 July 2022; Accepted 8 August 2022
Available online 14 August 2022

Medical staff could also experience electrostatic shock when exposed to the medical equipment since their body can get electrostatically charged easily in the OR at low relative humidity levels [7,8]. The electrostatic discharge from medical staff could also lead to the malfunction of electromedical devices and jeopardise the safety of patients [9]. The most frequently reported medical devices affected by electrostatic discharge include clinical chemistry analyzers, infusion pumps and heart assist devices [10]. In contrast, high relative humidity levels enhance the growth of mildew and mould on ceilings, walls, and even in air vents, which increases the risks of wound infection in patients [11,12].

The OR must retain a positive or higher pressure than the adjacent vicinity or environment [13]. This ensures that the air flows from a cleaner environment. The OR pressure should be maintained at +25 Pa to conserve the favourable pressure gradient in the adjacent vicinity (−2.5 Pa) [14,15]. The air should flow in from the ceiling and exit near the floor area to promote unidirectional laminar flow of air, whereby the velocity of airflow is between 0.3 m/s and 0.5 m/s [16–18]. Under unidirectional laminar flow, airborne contaminants are forced to traverse through the OR, impede wound harbouring as opposed to turbulent airflow and thus, generate an ultraclean operation area [19]. The movement of medical staff within the OR must be restricted during medical operations [20]. If medical staff create any unnecessary movement, the intended airflow within the OR will be disturbed, and the air contaminants cannot traverse correctly as intended [21]. The ventilation system of the OR operates at 15 to 20 air changes of filtered air per hour, while the adjacent vicinity operates at three air changes of filtered air per hour [22–24]. All medical staff must wear scrubs before entering the OR. This is because scrubs are made from antimicrobial materials that can be washed and cleaned easily [25]. Antimicrobial materials offer protection and prevent the growth of mould, mildew, and bacteria [26,27]. Therefore, pathogens cannot attach to scrubs, thus reducing the risk of transferring pathogens from clothing to wound.

Surgical site infections (SSI) are defined as infections that occur at the incision site within 30 days of the surgical procedure [28]. SSIs have been identified as a significant issue in an OR. Such infections can be superficial or deep incisional infections, as well as infections involving organs and body cavities [29]. It is considered a superficial incisional infection if it only involves the epidermis, dermis, and subcutaneous tissues [30]. However, if the infection affects deep tissues such as muscle and fascial layers, then it is considered a deep incisional infection [30]. SSI is significantly correlated to high morbidity and mortality rates. Patients experiencing SSI have high fatality rates, a 60% chance of being warded into the intensive care unit (ICU), and more than quintuple chances of readmission to the hospital after discharge [31]. Research studies have also shown that developing countries record higher SSI rates, ranging between 1.5% and up to as high as 21% of documented cases, compared to developed countries [32]. The data indicates that there is a crucial need to reduce the risk of SSI among patients in developing countries.

Airborne particles are characterised by low density, invisibility, and susceptibility to turbulence. The settlement of infectious airborne particles on a patient's wound can cause SSI. Coagulase-negative *staphylococci* (CoNS), which reside on human skin [3], are the most frequently detected bacteria in SSI [33], as well as *Mycobacterium chimaera* (*M. chimaera*) from the exhaust of heat-cooler units (HCU) [34]. *Staphylococcus aureus (S. aureus)*, which is commonly found on the human skin, armpit, groin, and nose [35], is generally considered the most common cause of SSIs in ORs [36,37]. Colony-forming unit (CFU) estimates the number of viable bacteria or fungal cells that can multiply via binary fission [38]. It has been reported that the CFU of CoNS $\geq 10^3$ can cause catheter-related bloodstream infections (CRBSI) [39]. Chand et al. studied the possibility of *M. chimaera* infection due to cardiopulmonary bypass HCU [40]. An aerobiological investigation was conducted by manipulating the water circulation process of the HCU. It was observed that 10 CFU/m^3 of bacteria was detected in the air when the water circulation was turned off. Once the water circulation was turned on, the number of bacteria shot up to 560 CFU/m^3 and *M. chimaera* was detected from both samples for on/off the water circulation. It was inferred that patients might be infected by *M. chimaera* due to aerosol contamination from the water tank of the HCU used during cardiopulmonary bypass. Hamza et al. [41] investigated the possibility of chronic and recurrent bone infection due to *S. aureus* and observed that 10^2 CFU of the microbes could cause acute bone infection.

The study by Agirman, Cetin, Avci and Aydin [28] showed that using an appropriate ventilation system could rapidly reduce the particle concentration. There are two main airflow principles applied in OR, namely, turbulent and laminar airflow systems [42]. The most common ventilation system used in modern ORs is unidirectional airflow ventilation (UAV), which is a uniform downward airflow system. The UAV system is more efficient in reducing the particle load of the air in the patient's proximity compared to the turbulent ventilation system [43,44]. Typically, the clean zone provided by UAV systems is crowded with medical staff and furniture; hence, some sterile instruments may be outside the protected area [45]. Mobile air supply (MAS) units are relatively convenient and easy to use. It can be easily repositioned to provide a specific region with low particle concentration. MAS unit is also designed for transporting sterile products under ISO Class 5 particle-free work area to ensure the integrity of products. According to Barnes, Twomey, Carrico, Murphy and Warye [34], MAS improves air quality in the OR by filtering airborne particles including surgical smoke-related particles.

The primary purpose of additional air treatment is to reduce the stagnant airflow region, enhance infectious particles removal, and provide a comfortable indoor environment for the patient and medical staff [46]. Recent studies by Sadrizadeh and Holmberg [37], Sadrizadeh, Holmberg and Nielsen [47], Sadrizadeh, Tammelin, Nielsen and Holmberg [48] found that an additional MAS unit could reduce SSI rates and decrease the number of viable airborne particles. Pasquarella, Sansebastiano, Ferretti, Saccani, Fanti, Moscato, Giannetti, Fornia, Cortellini, Vitali and Signorelli [49] experimentally assessed the efficacy of a MAS unit in reducing the concentration of the particles in an OR under a turbulent ventilation strategy during a proper abdominal surgical procedure. The average particle sedimentation on the instrumental table was reduced by 88.83%, from 2730 CFU/m^2/h to 305 CFU/m^2/h. Another study also found that the MAS unit contributed to a significant reduction in the mean count of sedimenting bacteria from 775 CFU/m^2/h to 355 CFU/m2/h on the patient's chest [50]. Other relevant findings on the application of a MAS unit, together with the methodology of the respective study, have been summarized in Table 1.

To the best of the authors' knowledge, past studies have highlighted the capability of the MAS unit in reducing the bacteria concentration within the OR. However, some recent studies have reported the conflicting effects of MAS units on the sterility of an OR [45,54]. The airflow supplied from the MAS unit could modify the local flow circulation pattern and may induce higher levels of bacterial contamination in other zones of the room [45]. This study also warned of the risk of simply installing a MAS unit in an OR without verifying the impact under different working conditions. Recently, Bluyssen, Ortiz and Zhang [54] claimed that the use of the MAS unit does not necessarily improve the contamination outcome, but the performance is dependent on the position, height and velocity supplied by the MAS unit. Sadrizadeh, Afshari, Karimipanah, Håkansson and Nielsen [55] also observed that the posture of medical staff could deteriorate the performance of the MAS unit. To date, research on the effect of airflow supplied by the MAS unit associated with particle dispersion is lacking, particularly comprehensive investigations using the numerical approach. Therefore, the objective of this study is to evaluate the effectiveness of the MAS unit in reducing the number of particles settling on a patient under different air velocities using a validated CFD model.

Table 1
Methodology and findings of relevant research on the application of MAS unit.

Reference	Methodology	Indoor/ Ventilation types	Finding
Tacutu et al. [51]	PIV and CFD	Indoor: Operating Room Main Ventilation: Unidirectional Airflow Ventilation	The velocities from the MAS unit must be at least 0.1 m/s higher than the general ventilation system to avoid disturbances generated from the main ventilation system
Vogelsang et al. [33]	Microbiological sampling	Indoor: Operating Room Main Ventilation: Conventional Turbulent Ventilation	MAS unit reduces CFU during neurosurgery to ultraclean air levels ($\leq$10 CFU/m^3) with an airflow velocity of 0.4 m/s to 0.5 m/s.
Thore and Burman [52]	Microbiological sampling	Indoor: Operating Room Main Ventilation: Turbulent Ventilation	The reaching distance of ultra-clean air of MAS unit is up to 1.5 m, independent of the type of turbulent ventilation.
Friberg et al. [53]	Microbiological sampling	Indoor: Operating Room Main Ventilation: Conventional Turbulent/ Mixing Ventilation	There was approximately 80% reduction in the bacterial count at a distance of 1.4 m−1.6 m from the MAS unit
Sadrizadeh & Homberg [37]	CFD	Indoor: Operating Room Main Ventilation: Turbulent Mixing Ventilation	The increase in MAS supplied-air velocity from 0.4 m/s to 1.0 m/s has no obvious or reverse effect on the particle impingement over surfaces.
Pasquarella, Sansebastiano, Ferretti, Saccani, Fanti, Moscato, Giannetti, Fornia, Cortellini, Vitali and Signorelli [49]	Microbiological sampling	Indoor: Operating Room Main Ventilation: Conventional Turbulent Ventilation	The impact of the MAS unit is limited to the targeted area and does not influence other sites of the OR
Casagrande and Piller [45]	CFD	Indoor: Operating Room Main Ventilation: Vertical Laminar Airflow Ventilation	MAS unit maintains the sterility of the instrumentation table and induces higher bacterial contamination in the other zone

*PIV and CFD denote Particle Image Velocimetry and Computational Fluid Dynamics, respectively.

2. Methodology

2.1. Description of the CFD model of an operating room

The OR has a dimension of 6.00 m (L) × 5.50 m (W) × 3.00 m (H). The clean air was supplied into the room through the ceiling-mounted air supply diffusers that have an effective surface area of 4.32 m^2. The outgoing air was extracted via the four exhaust grilles placed on the four corners of the wall at the height of 0.25 m above the floor level. Each of the exhaust grilles has a dimension of 0.22 m (W) × 0.46 m (H) with an effective surface area of 0.10 m^2. There were two doors modelled into the computational domain, with a dimension of 1.10 m (W) × 2.50 m (H). Some assumptions have been made as suggested by previous studies [55,56]: (i) the effect of the door's gap on airflow changes is assumed to be negligible, (ii) the particles were released by the medical staff members only, (iii) no intrusion of particles via the door gap since the room is in positive pressurization, (iv) no intrusion of particles from the air supply diffuser.

A total of six medical staff members were positioned around the operating table in an upright standing posture. A patient was placed on top of the operating table in a lying-down posture. Among the six medical staff members, three with bent-forearm were considered to perform the surgical procedures or prepare surgical tools for the surgeons, while the other three members with straight-forearm were assumed to assist and observe the surgical procedure. The OR was furnished with two sets of medical equipment, an instrument table, two surgical lamps, an operating table and a MAS unit. The operating table was placed at the centre of the room, while the instrument table was located beside the operating table at a gap distance of 1.10 m. The MAS unit was placed near the operating table. Each MAS unit was adjusted to supply clean air to the operating table. The MAS unit that was placed near the operating table has a dimension of 0.46 m (L) × 0.36 m (H) and was positioned at the height of 0.95 m above the floor level. Two surgical lamps were installed on the ceiling that provides lighting to illuminate the surgical site for optimal visualization and aid the surgeons during surgical procedures. The CFD model of an OR utilized in the present study is shown in Fig. 1. The OR model and the layout of furniture were obtained from previous studies [37,57,58]. Some modifications to the furniture arrangement were done to best fit the realism of the actual OR scenario.

Table 2 shows the detailed dimensions of various furniture and human manikins in the OR.

2.2. Verifying the grid independency

For indoor airflow simulation, the mesh must be sufficiently fine to resolve the field reliably of turbulent flow. In this study, a mesh refinement was applied to the regions with high gradients of transported quantities, such as air supply openings, exhaust grilles, MAS unit, instrument table, surgical lamps, two medical equipment, and all human manikins. Coarser elements were utilized in the remaining sections of the computational domain. The "*fixed*" option was activated under the advanced size function (ASF). The purpose of activating the ASF was to control the growth and distribution of the mesh in essential regions, i.e., curvature region or close proximity of surfaces. The maximum face size and maximum size of the mesh element were both adjusted to achieve a good quality mesh. A growth rate of 1.20 was applied between the mesh layers to obtain a reliable prediction of boundary layers in the near-wall region [57].

In this study, unstructured tetrahedral elements were utilized to mesh the computational domain of the OR. The unstructured mesh is typically used to optimally accommodate the complex geometry [59]. According to Bern and Plassmann [60], an unstructured mesh is one in which the local neighbourhood of vertices fluctuates arbitrarily. The advantages of unstructured tetrahedral elements include unique linear interpolation from vertices to the interior, increased flexibility in fitting challenging domains, and simplicity of refinement and derefinement [60]. Apart from tetrahedral elements, there are also unstructured hexahedral element meshes. The unstructured hexahedral element meshes are not considered in the study as it has more disadvantages than unstructured tetrahedral element meshes in terms of stress analysis [60].

The verification of mesh independence, also known as the grid-independent test (GIT), was performed to ensure that the numerical errors on the simulated results are negligible [32]. GIT is associated with the reliability or rationality of simulated results [139]. In the present

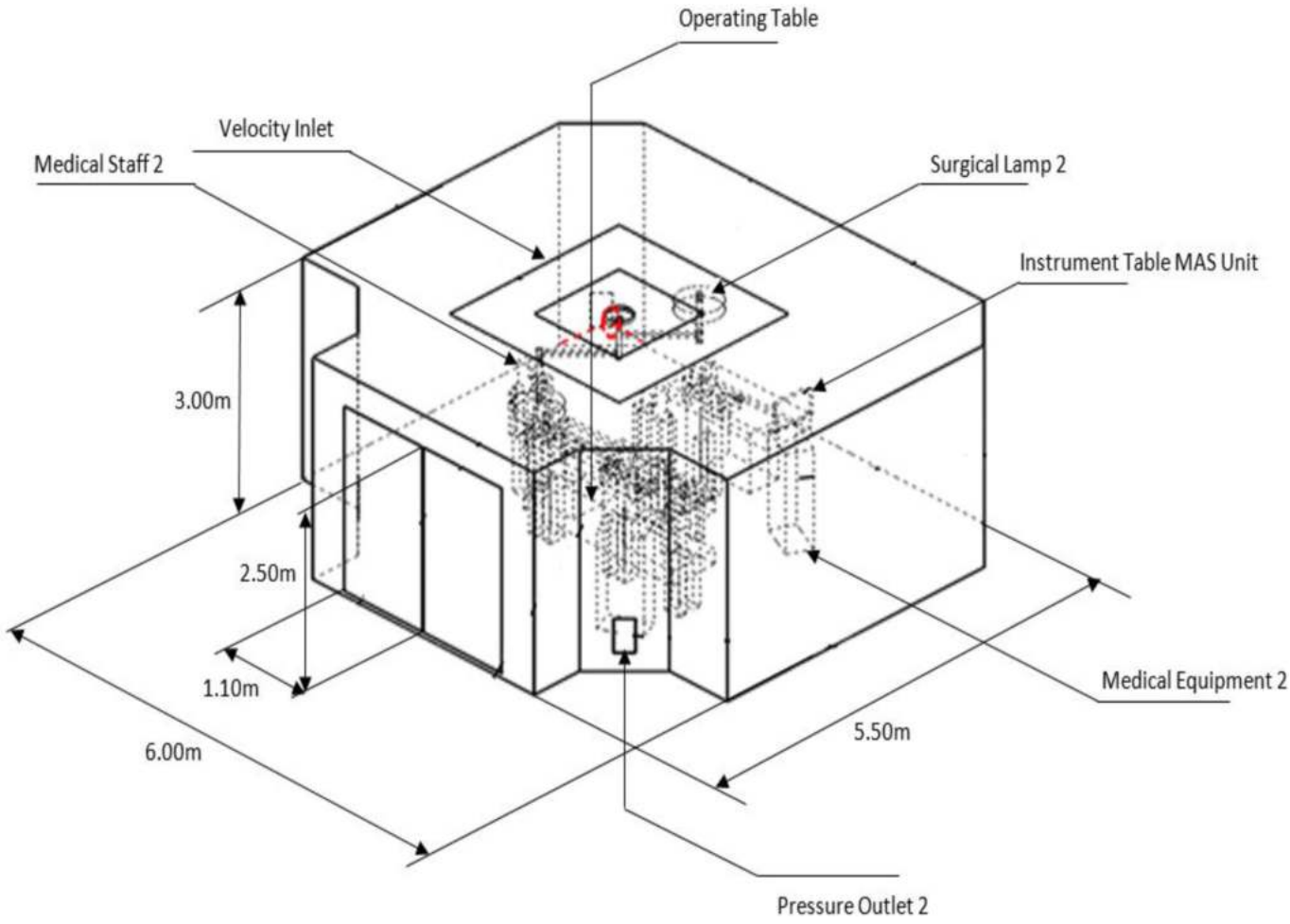

Fig. 1. CFD model representing a fully furnished OR used in the case study.

Table 2
Detailed dimensions of human manikin and furniture in the OR.

Symbol	Objects	Dimension (m)
OR	Operating room	6.00 (L) × 5.50 (W) × 3.00 (H)
V_i	Air supply diffuser (Velocity inlet)	Effective area: 4.32 m^2
P_o	Exhaust grilles (Pressure outlet)	0.22 (L) × 0.42 (H)
OT	Operating table	2.10 (L) × 0.60 (W) × 0.90 (H)
IT	Instrument table	1.40 (L) × 0.60 (W) × 1.00 (H)
OT_MAS	Operating table MAS unit	0.46 (L) × 0.36 (H)
SL	Surgical lamp	0.52 (D) × 0.13 (T)
ME	Medical equipment	0.50 (L) × 0.30 (W) × 1.35 (H)
D	Door	1.10 (W) × 2.50 (H)
MS	Medical staff	Body 0.30 (L) × 0.20 (W) × 0.675 (H) Head 0.15 (L) × 0.20 (W) × 0.305 (H) Hand 0.10 (L) × 0.10 (W) × 0.575 (H) Leg 0.10 (L) × 0.20 (W) × 0.75 (H)
P	Patient	Body 0.30 (L) × 0.20 (W) × 0.675 (H) Head 0.15 (L) × 0.20 (W) × 0.305 (H) Hand 0.10 (L) × 0.10 (W) × 0.575 (H) Leg 0.10 (L) × 0.20 (W) × 0.75 (H)

**L, W, H, D, and T denote length, width, height, diameter, and thickness, respectively.

computational domain of OR, the GIT was performed with six different sets of elements, ranging from 0.8 million to 2.4 million elements. Two different observing lines, which are lines X-X and Z-Z that penetrated through the computational domain, were selected. The line X-X connected the coordinates of (0.0, 0.8, 1.375) and (6.0, 0.8, 1.375), while the line Z-Z connected the coordinates of (3.0, 0.8, 0.0) and (3.0, 0.8, 5.5). The fluctuations of airflow velocities on 100 evenly distributed points along lines X-X and line Z-Z were plotted in Fig. 2 (a) and (b).

The grid convergence index (GCI) was calculated to determine the discretization error of the grid independence test. A small GCI indicates that the discretization error is sufficiently small and approaches the true numerical solution [61]. The grids are sufficiently fine, and the numerical error is negligible when the values of GCI are <5% [62,63]. The GCI can be computed via Equation. (1) described in Paudel and Saenger [64]:

$$GCI(u) = \frac{F_s \varepsilon_{rms}}{r^p - 1} \quad (1)$$

Where F_s is the safety factor, ε is the relative difference, p is the order of convergence, and r is the refinement factor between the fine and coarse mesh.

The ε_{rms} is defined as shown in Equation (2):

$$\varepsilon_{rms} = \sqrt{\frac{\sum_{i=1}^{n}\left[\frac{u_{i,coarse} - u_{i,fine}}{u_{i,fine}}\right]^2}{n}} \quad (2)$$

Where u_i is the airflow velocity and n is the number of sampling points.

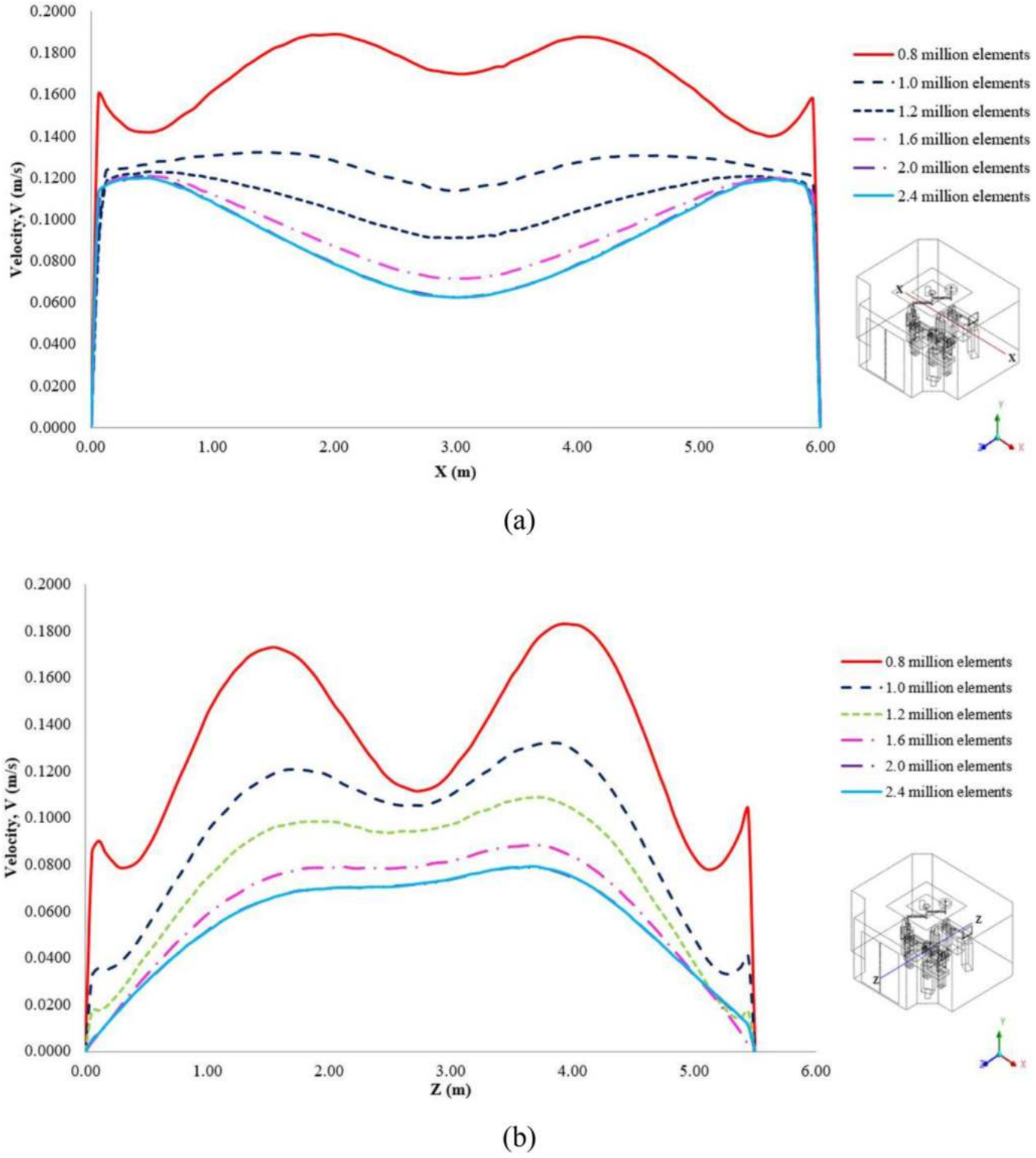

Fig. 2. Variation of airflow velocity magnitudes on 100 evenly distributed points for six different sets of mesh density along (a) line X-X, (b) line Z-Z.

The present study found that when 2 million elements were used, the GCI was 4.9% and 4.7% on the lines X-X and the line Z-Z, respectively. Therefore, 2 million elements were used for subsequent case studies.

2.3. Setting up the boundary conditions and prescribing the fluid and particle properties

An inlet airflow condition was specified at the ceiling-mounted air supply diffusers at a velocity and turbulent intensity of 0.43 m/s and 5%, respectively. All airflow boundary conditions were specified in the direction perpendicular to the respective surfaces. The reason is that the air supplied from the face area of the air supply diffuser is in a unidirectional manner. Each exhaust grill was set as the Neumann boundary condition with a zero-gauge pressure. The airflow inside the OR was assumed to be incompressible and at constant density. With a no-slip condition applied to all interior walls, the fluid is expected to adhere

to the wall, and the airflow velocity gradually increases when further away from the walls [57]. An RNG k-epsilon turbulence model was selected while the enhanced wall treatment function was activated. The purpose of the enhanced wall treatment is to provide good airflow and particle dispersion in near-wall regions. The averaged velocity and turbulent intensity of each MAS unit were set at 0.4 m/s and 5%, respectively, as suggested by Sadrizadeh, Tammelin, Nielsen and Holmberg [48]. The gravitational force acted in a downward direction with an acceleration of 9.81 m/s^2.

The consideration of heat fluxes released by objects is significant as it could disrupt the airflow distribution in the operating room and consequently affect particle transportation [56]. In the present study, the heat flux released by the six medical staff members, the patient, the surgical lamps and the medical equipment was considered. The heat flux values were obtained from the study conducted by Sadrizadeh, Afshari, Karimipanah, Håkansson and Nielsen [55]. Each medical staff released a heat flux of 116 W/m^2, while the patient released a lower heat flux of 58 W/m^2 as there was no physical movement performed. All walls in the OR were treated adiabatically due to the negligible temperature difference between the air and walls.

For the particle boundary condition, an escape condition was set on the air supply diffuser, exhaust grilles, medical staff members and MAS units. A trap condition was specified at the operating table, instrument table, surgical lamps, medical equipment, doors, floor, interior walls, and patient. Each medical staff member released particles at a rate of 600 particles/min from their exposed surfaces (equivalent to a mass flow rate of 1.31×10^{-12} kg/s) [65]. With a diameter ranging from 5 μm to 10 μm, the airborne particles are basically considered bacteria-carrying particles [66]. According to Liu, Wang and Wen [65], the predicted particle distribution using a particle diameter of 5 μm was almost similar compared to using a particle diameter of 7 μm or 10 μm because of negligible differences in size and density of the particles. Hence, the particle diameter of 5 μm with a density of 2.0 g/cm^3 was applied [65]. The dispersion of particles due to turbulence was modelled using the Stochastic tracking feature. Table 3 shows the boundary conditions prescribed on the CFD model of the OR.

Table 3
Detailed boundary conditions prescribed on CFD model of OR.

Location	Boundary conditions	Setup
Air supply diffuser	Velocity inlet	**Velocity magnitude:** 0.43 m/s **Direction of airflow:** Normal to the boundary **Turbulent intensity**: 5% **Temperature:** 292 K (19 °C) **DPM:** Escape
Exhaust grilles	Pressure outlet	**Gauge pressure:** 0 Pa **DPM:** Escape
Medical staff 1 - 6	Wall	**Wall motion:** Stationary wall **Wall condition:** No-slip **Heat flux:** 116 W/m^2 **DPM:** Trap
Patient	Wall	**Wall motion:** Stationary wall **Wall condition:** No-slip **Heat flux:** 58 W/m^2 **DPM:** Trap
Operating table/Instrument table/Door/Floor/Interior walls	Wall	**Wall motion:** Stationary wall **Wall condition:** No-slip **Heat flux:** 0 W/m^2 **DPM:** Trap
Mobile air supply unit	Velocity inlet	**Velocity magnitude:** 0.1–0.6 m/s **Direction of airflow:** Normal to the boundary **Turbulent intensity**: 5% **DPM:** Escape
Surgical lamp	Wall	**Wall motion:** Stationary wall **Wall condition:** No-slip **Heat flux:** 320 W/m^2 **DPM:** Trap
Medical equipment	Wall	**Wall motion:** Stationary wall **Wall condition:** No-slip **Heat flux:** 255 W/m^2 **DPM:** Trap

2.4. Case studies

The present study included the MAS unit for additional clean air supply in the OR. The aim was to also assess its effectiveness in reducing the number of particles that settled on the patient. Previous studies justified that air supply velocity from the MAS unit needs to be higher by at least 0.1 m/s to overcome the interruptions generated from the main laminar airflow system in an OR [67]. Thus, this study also examines the airflow profile resulting from different air velocities supplied from the MAS unit, ranging from 0.1 m/s to 0.6 m/s. A total of 6 case studies were performed on the MAS unit with different supply air velocities, as presented in Table 4. The purpose was to examine the ideal air supply velocity that could achieve the maximal reduction of particle concentration at the surgical site.

The present study modelled the air supply diffuser of MAS unit using the fan boundary condition, by considering the polynomial profile. To ensure that the supplied air is free of particle along the axial fan rotor, a "trap" condition under the discrete phase model of MAS unit boundary was prescribed. Such setup on the MAS unit has been utilized in the previous studies and proven to be reliable [37,68]. The MAS diffuser's screen has a dimension of 0.46 m (length) × 0.36 m (height), contributing to an effective area of 0.1656 m^2. The air temperature supplied by the MAS unit's diffuser was 19 °C, which is the recommended air temperature for an OR [69]. The density, kinematic viscosity, and pressure of the air were set at 1.20 kg/m^3, 0.0000497 m^2/s, and 101 kPa, respectively. Referring to Table 4, the MAS unit in each case study has a different Reynolds number ranging from 2698 to 16,188. However, all these values fall under the requirement of a MAS unit, which is to supply a unidirectional airflow condition (laminar airflow region). The location of the MAS unit with respect to the patient is shown in Fig. 3.

Table 4
Supplied air velocity from the MAS unit in each case study.

Case Study	Supplied air velocity (m/s)	Reynolds number (Re)	Supplied air temperature (°C)	Turbulent intensity (%)
1	0.1	2698	19	5
2	0.2	5396	19	5
3	0.3	8094	19	5
4	0.4	10,792	19	5
5	0.5	13,490	19	5
6	0.6	16,188	19	5

2.5. Validation of airflow velocity and particle concentration in patient ward

A thorough validation of airflow velocity and particle concentration was performed before the baseline case. The field measurement data collected by Zhao, Yang, Chen, Feng, Yang, Sun, Gong and Yu [62] in an ISO class 5 patient ward was selected. The reason is that the indoor airflow condition is similar to the airflow condition in an operating room. The validation of turbulent models was conducted under a steady-state condition. The patient ward has a floor area of 10.23 m^2 (3.3 m (L) × 3.1 m (W)) and a floor-to-ceiling height of 2.5 m. The patient ward was partitioned into two compartments: a patient care area and a bathroom. The bathroom compartment has a volume of 5.25 m^3,

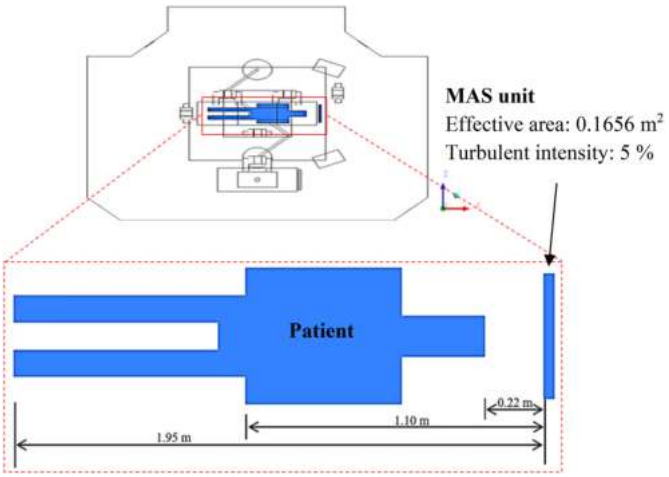

Fig. 3. Location from MAS unit to the patient.

while the patient care area has a volume of 20.15 m^3. The first air supply opening was on the bathroom ceiling, while there was a thin-thickness opening located in the space between the floor and the door separating these two sections. The clean air was supplied through a horizontal inlet with the dimension of 0.5 m (L) × 0.5 m (W) in the bathroom, creating a wind curtain that stops contaminants from entering the patient care area. In the bathroom, the overall dimensions of both toilet and particle generator were 0.4 m (L) × 0.4 m (W) × 0.4 m (H) as well as 0.35 m (L) × 0.3 m (W) × 0.55 m (H) respectively. The bathroom's air exhaust vent with 0.2 m (W) × 1.8 m (H) ran downward along the sidewall. The HEPA filter was also fitted to the ventilation system to supply clean air into the patient care area through a ceiling-mounted diffuser with a surface area of 7.5 m^2. The contaminated air was extracted through the five low-level wall-mounted air outlets. Each outlet has a dimension of 0.75 m (W) × 0.3 m (H). Fig. 4 shows the configuration of a patient ward that fulfilled the ISO Class-5 cleanroom [62].

A total of five turbulent models based on Reynold-Averaged Navier Stokes (RANS) were used to simulate the airflow velocity in the OR. The turbulent models were standard k-ε, RNG k-ε, realizable k-ε, SST k-ω, and standard k-ω. The simulated airflow results were then compared with the measured airflow data by Zhao, Yang, Chen, Feng, Yang, Sun, Gong and Yu [62]. Validation is claimed when the relative error between the simulated result and measured data is less than 10% [71].

As shown in Fig. 5, the averaged relative errors of RNG k-ε, realizable k-ε and standard k-ε are 8.54%, 9.60% and 9.03%, respectively. The airflow predicted using a standard k-ω model may have over/under predicted the actual airflow condition, with an averaged relative error of 11.82%. Therefore, the RNG k-ε model that predicts the airflow distribution more accurately was used for subsequent indoor airflow simulation. This airflow finding is in good consensus with the validation work performed by other researchers in the literature [72–74]. The comparison of the current simulated airflow velocity (RNG k-ε), measured airflow data, and simulated airflow velocity with the findings of Zhao, Yang, Chen, Feng, Yang, Sun, Gong and Yu [62] is shown in Fig. 6.

Based on Fig. 6, the simulated airflow velocity was close to the measured airflow velocity at four sampling points (x = 0.15 m, x = 0.90 m, x = 2.40 m, and x = 3.15 m). A large deviation was found between the simulated and measured velocity at the sampling point of x = 1.65 m. A similar deviation issue was also encountered by Zhao et al. (2009)

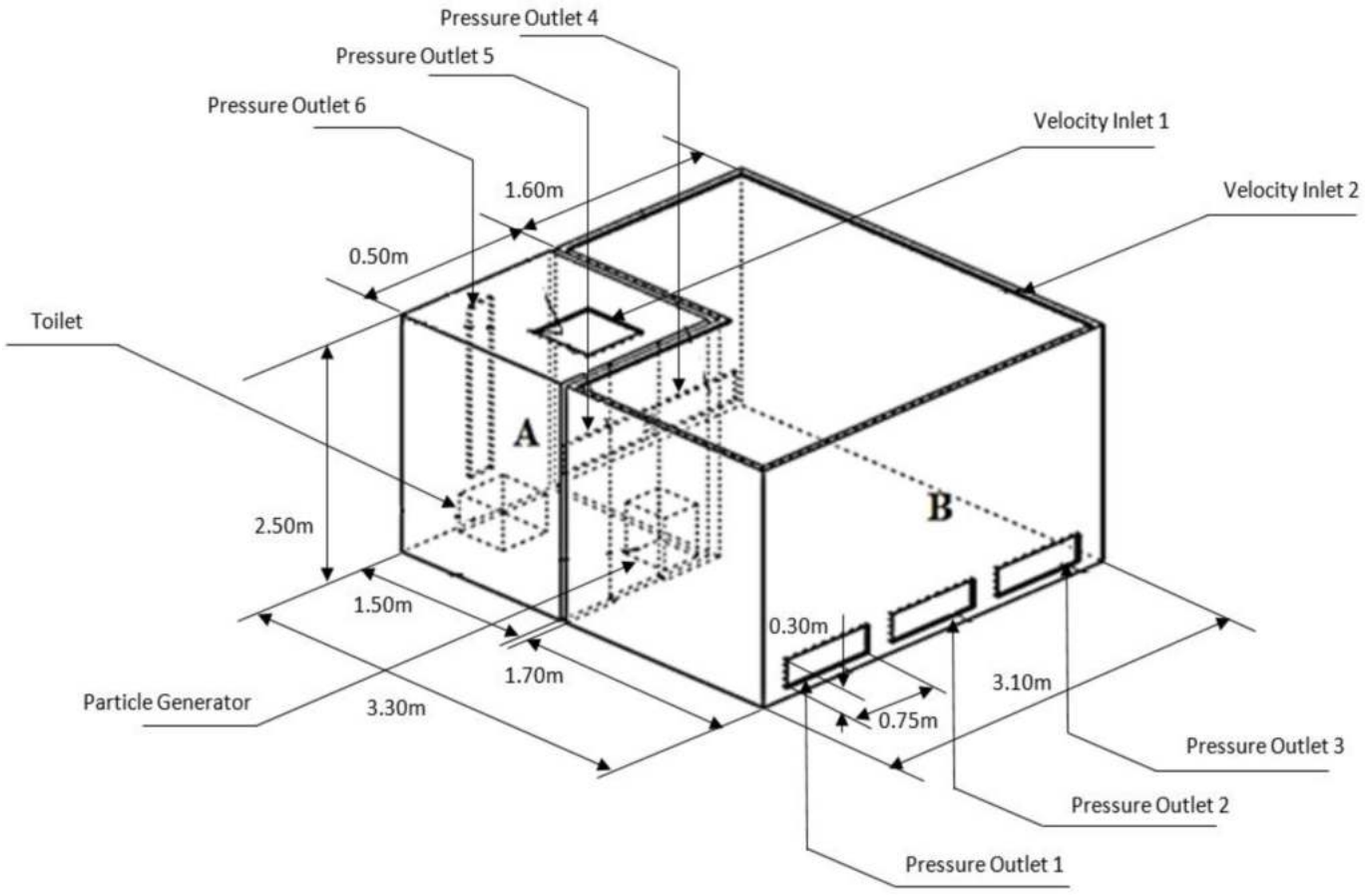

Fig. 4. Layout of an ISO class-5 patient ward for validation purposes [62].

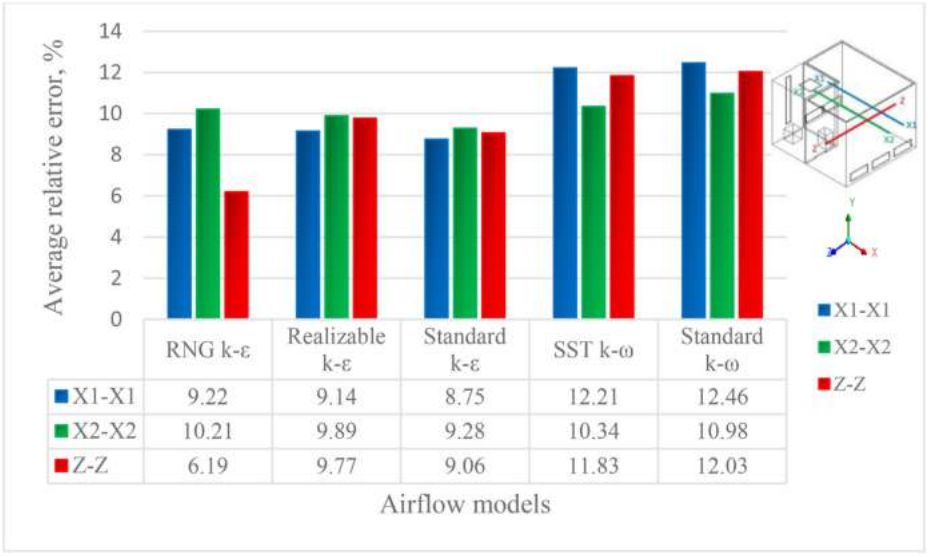

Fig. 5. Comparison of the average relative error between five turbulence models along lines X1-X1, X2-X2 and Z-Z.

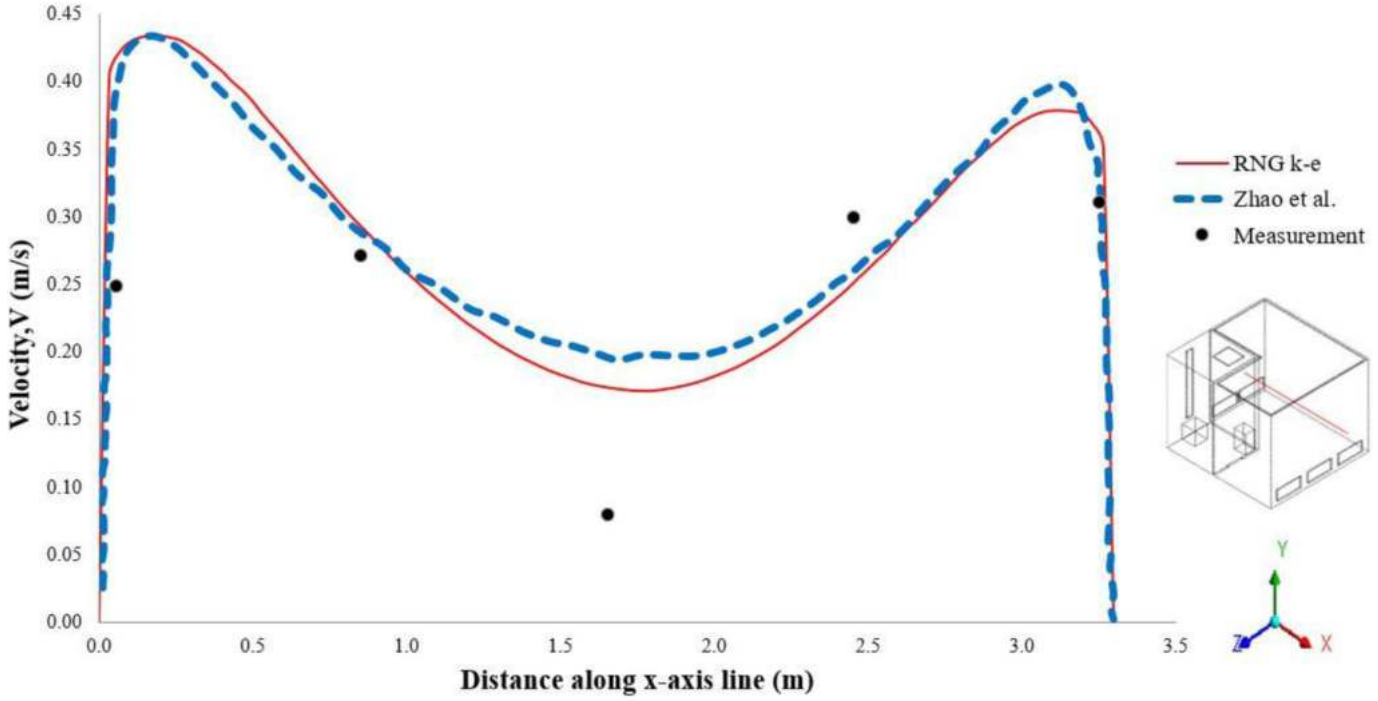

Fig. 6. Comparison of presently simulated, measured airflow velocity and simulated airflow velocity with Zhao et al. (2009) at the height of 0.8 m along line X1-X1.

[62] when the group performed the airflow simulation in the same computational domain. The authors identified that the logging of airflow data using the hot-sphere anemometer (Model: RHAT-301) was less accurate at airflow velocity below 0.1 m/s [62]. Hence, the measured airflow data at this point could be considered an outlier. In the present study, the simulated airflow has a good agreement with the simulated airflow by Zhao, Yang, Chen, Feng, Yang, Sun, Gong and Yu [62]. Likewise, the relative error between the simulated airflow and measured airflow by Zhao, Yang, Chen, Feng, Yang, Sun, Gong and Yu [62] was 8.54%, which was below the recommended value (<10%) for validation [75]. Hence, the airflow simulation was validated. To ensure that the simulated particle dispersion is reliable, validation of particle concentration based on a discrete phase model (Lagrangian approach) was utilized. Two different monitoring lines that show the variation of particle concentration along the distance of the Y-axis were plotted, namely, line P1 and line P2. The coordinates that connected line P1 and P2 are (1.10, 0.00, 2.75) and (1.10, 2.50, 2.75), as well as (0.70, 0.00, 2.75) and (0.70, 2.50, 2.75), respectively. The variations of particle concentration along lines P1 and P2 and their location are shown in Fig. 7.

The dimensionless particle concentration shown in Fig. 7 (a) and 7 (b) can be determined using Equation (3) [75].

$$C_{dim} = \frac{C}{C_{ref}} \tag{3}$$

where C_{dim} is dimensionless concentration, C is local particle concentration, and C_{ref} is reference particle concentration. Referring to Fig. 7

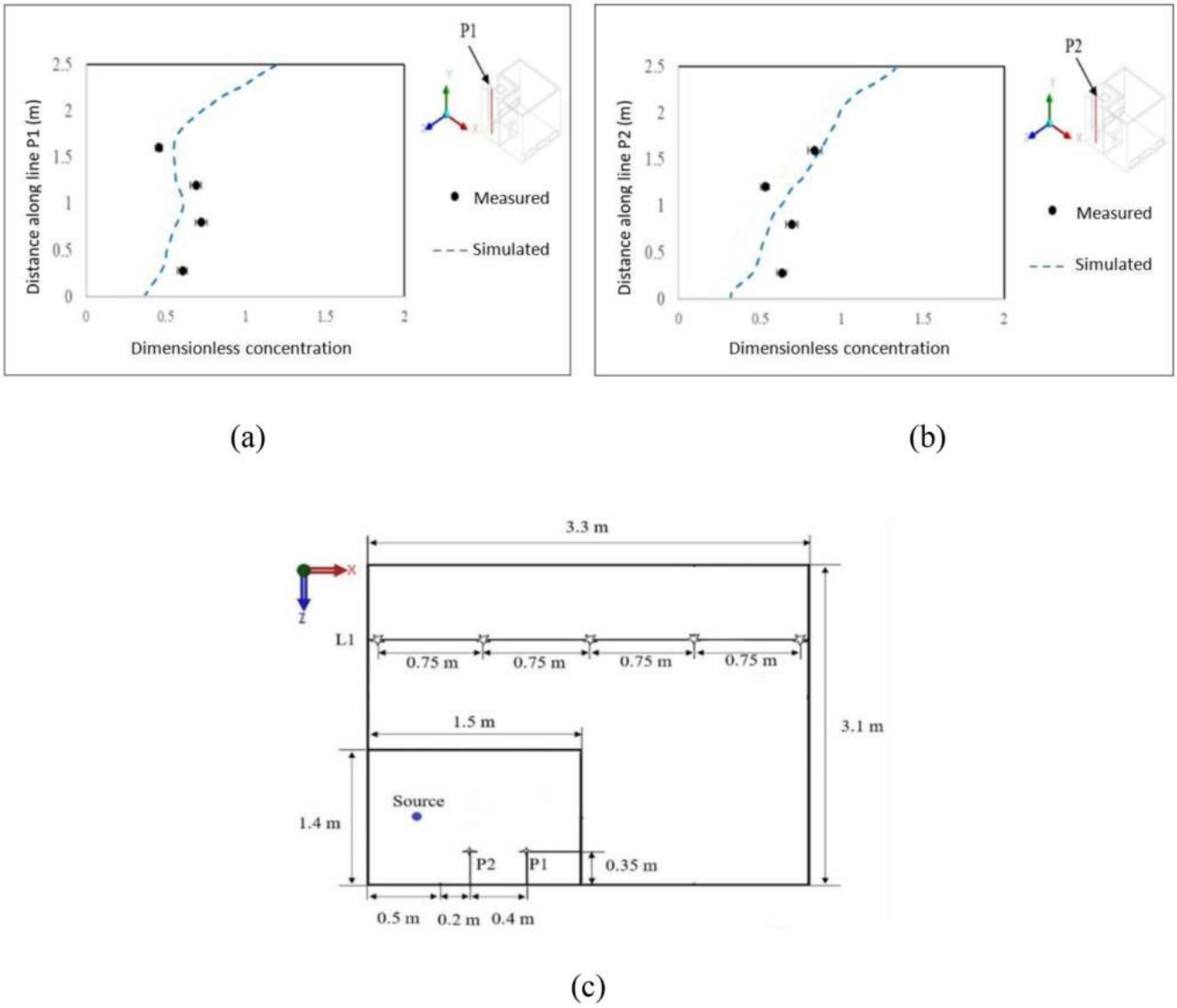

Fig. 7. Variation of particle concentration plotted along (a) line P1, (b) line P2, and (c) coordinates of P1 and P2 showing from plan view.

(a) and 7 (b), the deviation of the simulated concentration could be attributed to the particle leakage from the connection between the generator and pipe during experiments [62]. However, the simulated particle concentration results are close to the measured particle concentration with an average relative error of approximately 7.3%, which was within the allowable error range of 10% [57].

In general, the uncertainty of the simulated airflow distribution and particle concentration results was identified based on comprehensive verification and validation. The mesh independence was verified after achieving a GCI of <5% [62,63], while the simulated results were validated based on the relative error between the simulated and measured data falling, i.e., below 10% [57,71]. Hence, the CFD model is considered valid for subsequent analysis.

3. Results and discussion

3.1. Airflow and particle concentration without activating MAS unit

Under the present ventilation system, a high airflow region was observed in a downward direction near the air supply diffuser. The non-uniform airflow contour was observed around the medical staff members. A relatively low airflow distribution was identified in the region under the operating table due to the obstruction of the operating table. In addition, the thermal plumes rising from the patient collide against the downward airflow, which contributes to the lower air velocity in the region [76]. A noticeable swirling flow could be observed at the top corner of the OR, as shown in Fig. 8. Such airflow should be prevented as it could cause the surrounding airborne particles to penetrate the surgical zone. Referring to Fig. 2, the centre of the OR was not covered by the air supply diffuser. This region was used to mount the supporting structure of surgical lamps. Therefore, the air motion in the region right below this area was close to stagnant, mainly relying on the pressure difference with the adjacent region. Similarly, a small recirculation airflow could be observed in the region surrounding the support structure of the surgical lamp.

Referring to Fig. 8, the airflow distribution result indicates that the total air supplied into the room was not sufficient. Although the ventilation set-up and design layout have fulfilled the requirements as stated in ASHRAE Guidelines [77], the airflow distribution was relatively low after passing through medical staff members and obstacles. When the air reached the elbow of the staff, the airflow velocity was reduced to approximately 0.23 m/s. The worst scenario was that the impaired

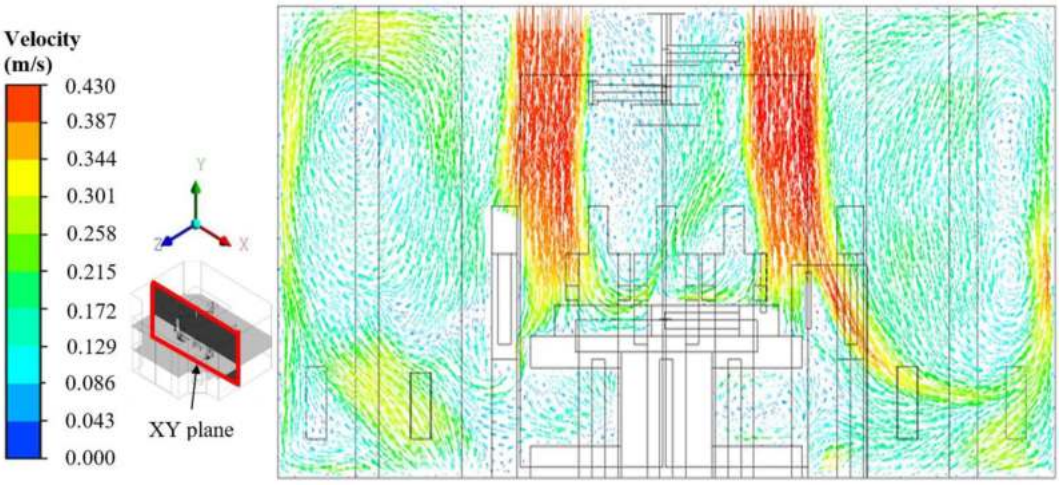

Fig. 8. Airflow velocity distribution on plane XY cut through the coordinate Z = 2.75 m, viewing in vector form.

airflow around the patient was almost stagnant with minimal to no air dilution. This phenomenon could promote the particles accumulated above the patient and increase the tendency of particles to settle on the patient's wound. The air velocity became close to zero while reaching near the floor level. Such a low airflow was not desirable in the OR, as it was incapable of transporting the particles to the exhaust grilles. Therefore, those settled particles tend to recirculate in the room when there is any induced airflow by medical staff members' movements.

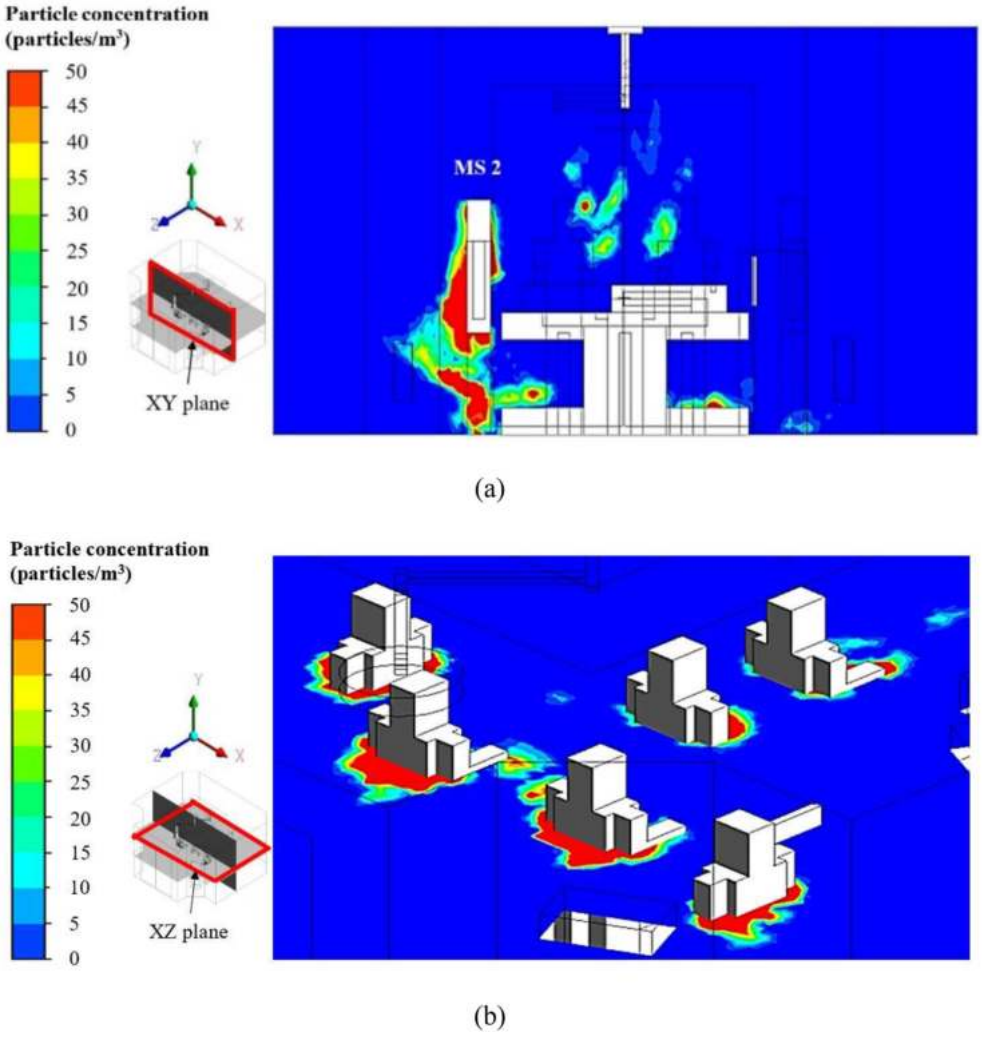

Fig. 9. Contour of particle concentration on (a) XY plane cutting through coordinate z = 2.75 m; (b) XZ plane cutting coordinate y = 1.18 m without operating MAS unit.

Referring to Fig. 9 (a), the gap between the medical staff trapped a high concentration of particles of approximately 48 particles/m^3. The particle accumulation was due to a stagnant airflow region, which resulted from the obstructions of the medical staff's upper body and the top surface of the operating table. Similarly, noticeable airborne particles were dispersed right above the patient with a distance ranging from 0.11 m to 0.64 m of the lying down the patient. The present study indicated that the air supplied from the air supply diffuser was inefficient, as it did not remove those particles in this region effectively. The obstruction of the operating table also contributed to the accumulation of particles below the operating table. Referring to Fig. 14 (b), the front part of the medical staff members has a low particle concentration, especially for MS 1, MS 3, MS 4, and MS 6. These medical staff members were standing right below the air supply diffuser layout. Hence, the clean air managed to wipe off the particles. However, a high particle concentration of 50 particles/m^3 was accumulated at the back of the medical staff members. This scenario was due to the heads of medical staff members, which blocked the clean air, thereby preventing the washing effect of air towards the back of the medical staff. For MS 3 and MS 4 with the bending forearm, who were assumed to perform surgical procedures, approximately 23–41 particles/m^3 were observed under the bent forearm. This finding is in good consensus with Kamar, Wong and Kamsah [57], where a noticeable particle concentration was accumulated under the bent forearm. Kamar, Wong and Kamsah [57] reported that these particles could increase the risk of infection when the medical staff member performed any dynamic movements, i.e., changing surgical tools, turning, or walking.

3.2. Airflow and particle concentration with activating MAS unit

The MAS unit was used as an additional air supply in the OR. The objective of utilising the MAS unit was to assess its effectiveness in removing the particle concentration around the patient and subsequently reduce the tendency of settlement on the patient. If the clean air is supplied far from the occupant, the distributed air has a higher probability of being polluted by the time it reaches the occupied zone. Therefore, the MAS unit was located at the height of 0.95 m above the floor level and the air diffuser was adjusted to directly face the patient at a distance of 0.22 m away from the head.

As seen in Fig. 10, the air supplied from the MAS unit was perpendicular to the air supplied from the ceiling-mounted air supply diffuser. With the activation of the MAS unit, the overall airflow distribution at the surgical site was increased to 0.31 m/s, especially in the region directly above the patient. Hence, the air dilution process occurred faster, and the particles were less likely to remain in the vicinity. This occurrence subsequently reduced the tendency of particles to settle on the patient. Evidently, the provision of a higher clean airflow rate that covers the operating microenvironment could be a practical approach to sweeping away the bacteria-carrying particles and preventing the development of SSI [76]. The contour of particle concentration on plane XY that cut through the coordinate of z = 2.75 m is shown in Fig. 11.

When the MAS unit was operated under the default air supply velocity of 0.4 m/s, a particle-free region was identified in the region above the patient. Such a contaminant-free region was extended from the MAS unit diffuser up to the patient's waist, with a total coverage distance of 0.704 m. Referring to Figures, 11 (a) and (b), the particle concentration reached a maximum value of 45 particles/m^3 and 11 particles/m^3 under the non-operated and operated MAS units, respectively. It can be claimed that the particle concentration was reduced by 78% when the MAS unit was switched on. This finding proved that the MAS unit could provide an efficient washing effect on the dispersed particles at the surgical site. A similar result was reported by von Vogelsang, Förander, Arvidsson and Löwenhielm [33], who demonstrated that the application of the MAS unit could reduce the airborne CFU to ultraclean level in the surgical field. However, the clean air supplied from the MAS unit could not cover the whole region above the patient. It could be observed that there were some particles dispersed in the region above the patient's leg. Similarly, a noticeable particle concentration of 28 particles/m^3 was identified under the operating table, close to the lower part of the support structure. The airflow velocity at the surgical site on the XZ plane that cuts through coordinate y = 1.18 m is presented in Fig. 12.

Referring to Fig. 12 (a), a swirling flow was formed near the bent forearm of medical staff members. The observation is similar to the wobble and recirculating streamline patterns produced under a low ventilation rate without the activation of the MAS unit [45]. Such undesirable airflow could trap and circulate the particles in this region instead of transporting them away from the surgical site for removal through the exhaust grilles. However, a more uniform airflow could be achieved in a similar region when the MAS unit was operated, as shown in Fig. 12 (b). The uniform airflow managed to sweep away the particles above the patient and subsequently reduced the tendency of particles to settle on the patient. Consequently, the risk of the patient getting a surgical site infection was also reduced.

3.3. Airflow and particle concentration under parametric studies

The present study also investigated the airflow distribution and particle dispersion under different airflow velocities supplied by the MAS unit. When the MAS unit supplied air with a velocity of 0.1 m/s up to 0.6 m/s, the airflow coverage distance extended from 0.242 m to 1.232 m toward the patient. Fig. 13 shows the airflow coverage distance against the air velocity supplied by the MAS unit.

As shown in Fig. 13, the increase in supplied air velocity from the

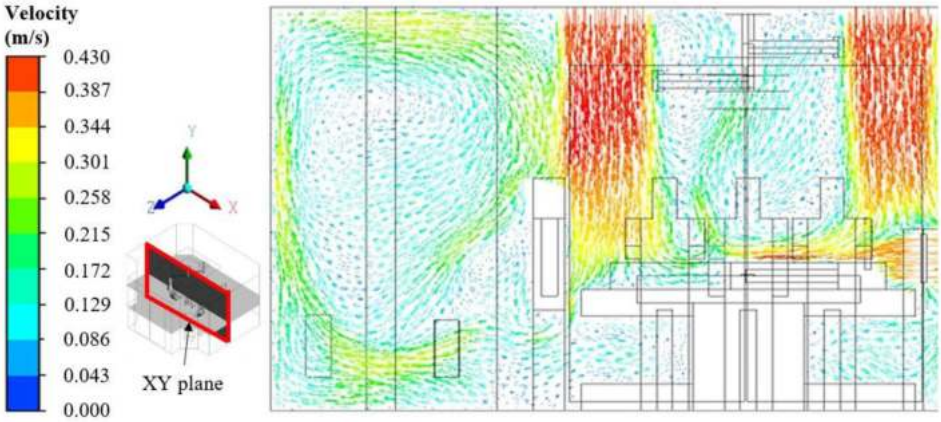

Fig. 10. Airflow velocity distribution with the activation of MAS unit on plane XY cut through the coordinate Z = 2.75 m, viewing in vector form.

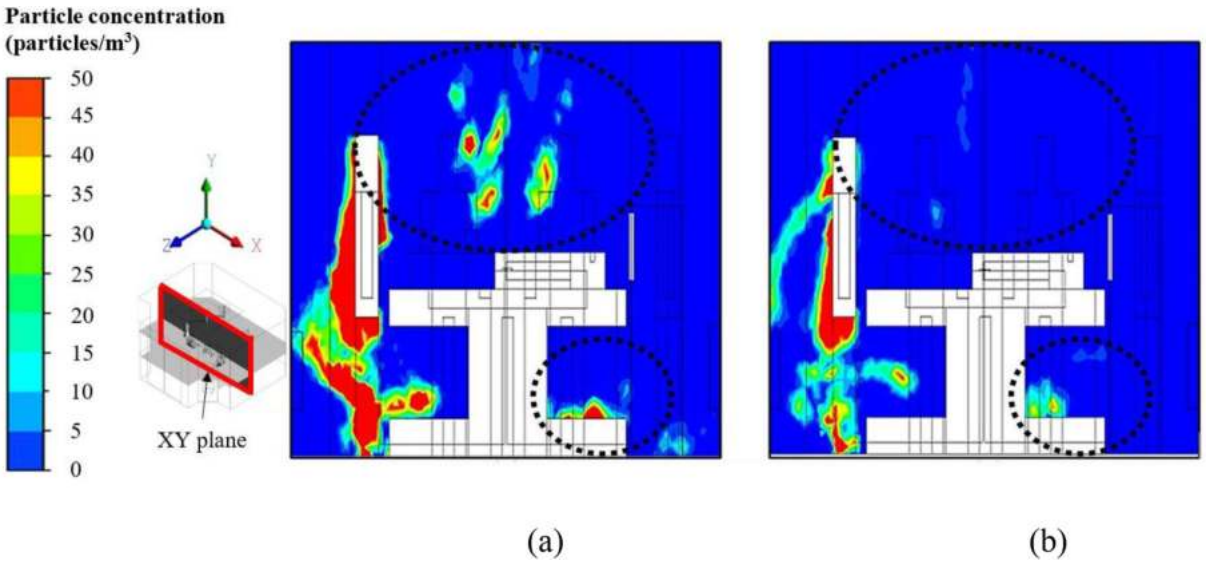

Fig. 11. Contour of particle concentration on plane XY cut through the coordinate Z = 2.75 m, under the condition of (a) not-operated MAS unit, (b) operated MAS unit.

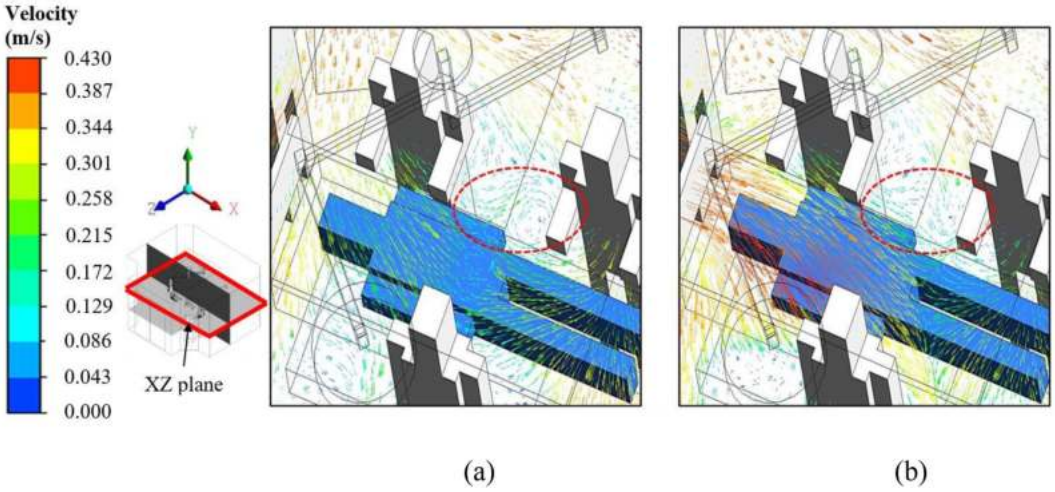

Fig. 12. Airflow velocity vector on XZ plane that cuts through the coordinate of y = 1.18 m under (a) non-operated MAS unit, and (b) Operated MAS unit.

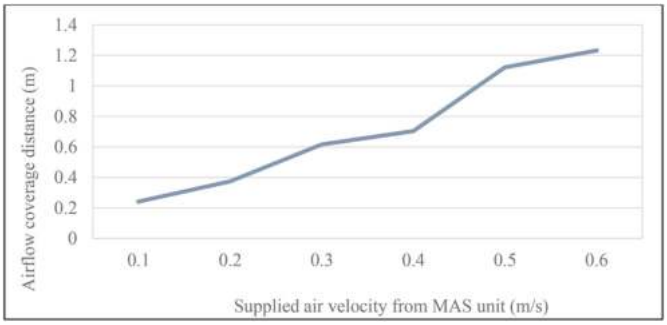

Fig. 13. Airflow coverage distance from the diffuser of MAS unit up to the patient under different supplied-air velocities.

MAS unit has increased the airflow coverage distance above the patient. The airflow coverage distance refers to the clean horizontal airflow zone that supplied from the MAS unit. A significant increment in the coverage distance could be noticed when the supplied air velocity increased from 0.4 m/s to 0.5 m/s. The plot in Fig. 13 indicated that if the supplied air increased to 0.5 m/s, the clean air could extend an additional coverage distance of approximately 0.4 m to remove the particles. In this context, The reaching distance of the laminar airflow supplied from the MAS unit could indicate the effective coverage distance of the contaminant-free area. This could be attributed to the stagnant region that is out of the reach of airflow, which allows the particles to persist in the surgical site [33]. The airflow distribution in the OR using different air velocities supplied from the MAS unit is shown in Fig. 14.

As seen in Fig. 14 (a)–(f), the red dotted circles highlighted the airflow coverage region supplied from the MAS unit. When the MAS unit delivered the air with a velocity of 0.1 m/s, the clean unidirectional air only managed to reach the patient's forehead. The airflow region extended to the patient's neck with the supplied air velocity of 0.2 m/s and 0.3 m/s. This range of velocities (0.1 m/s – 0.3 m/s) was insufficient to provide a satisfactory airflow region to ensure a low infection risk surgical procedure. Early epidemiological studies had pointed out that the high rate of open thoracic and abdominal SSI could cause substantial morbidity and mortality [78,79]. Therefore, a desirable airflow region should at least cover the critical chest and abdominal regions in standard operative procedures. A further increment in the air velocity of 0.4 m/s, 0.5 m/s, and 0.6 m/s could cover the region up to 0.707 m and 1.161 m

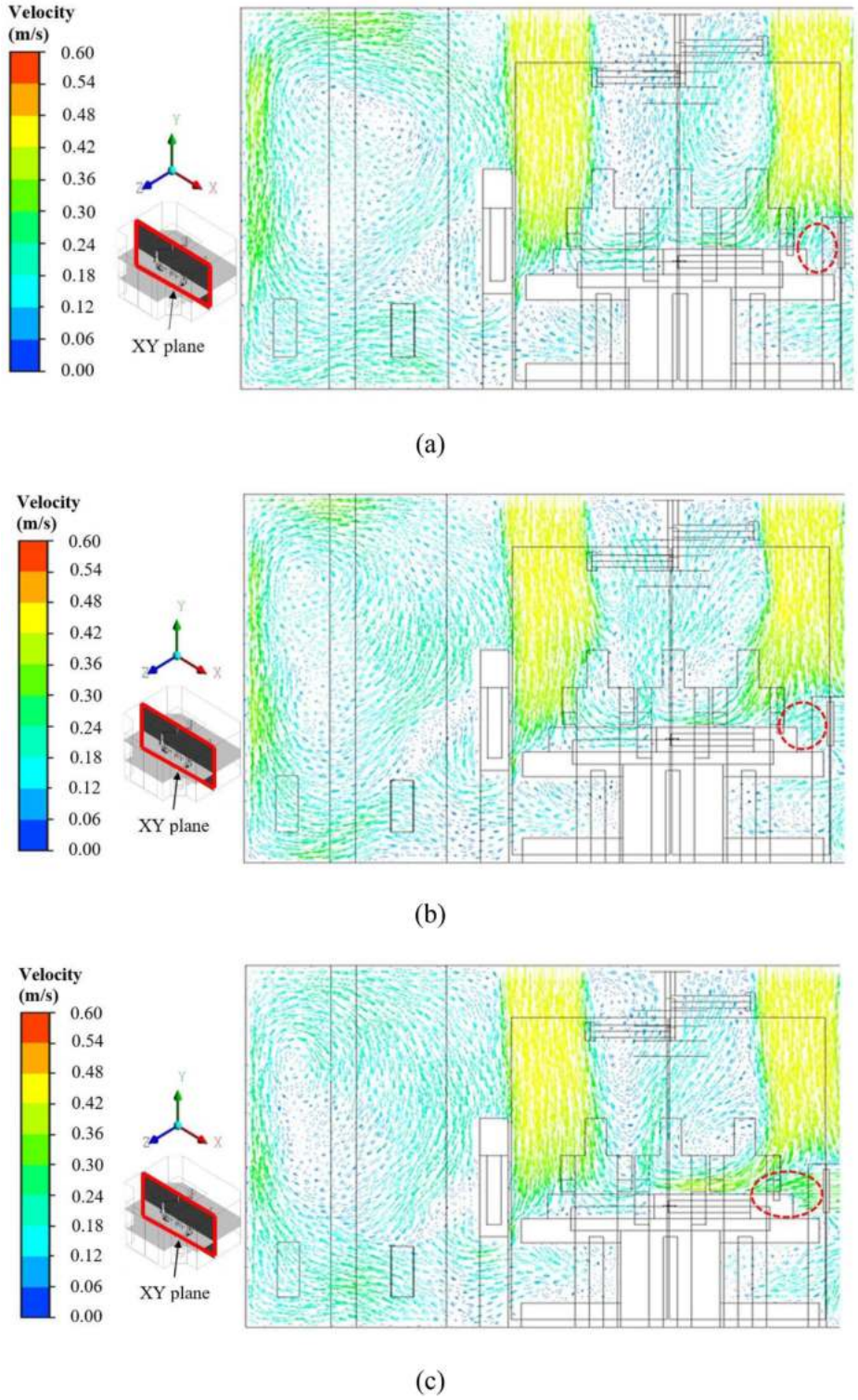

Fig. 14. Airflow velocity vector on XY plane that cuts through the coordinate of z = 2.75 m when the MAS unit supplied air at velocity of (a) 0.1 m/s, (b) 0.2 m/s, (c) 0.3 m/s, (d) 0.4 m/s, (e) 0.5 m/s, and (f) 0.6 m/s.

1.232 m, respectively. The present finding showed that supplied air velocity of 0.6 m/s could reach the patient's upper leg region. Hence, this velocity was considered the most effective supplied-air velocity if taking into account the coverage range. The particle concentration contours on the XY plane that cuts through the coordinate of z = 0.75 m using different supplied-air velocities are shown in Fig. 15(a–f).

When the MAS unit operates from 0.1 m/s up to 0.5 m/s, the particle concentration above the patient reduces gradually from 40 particles/m^3 to approximately 0 particles/m^3. However, increasing the supplied air velocity to 0.6 m/s displayed a reverse effect on the particle impingement (~7 particle/m^3) in the region above the patient. This occurrence could be attributed to the local vortices generated by the high velocity of

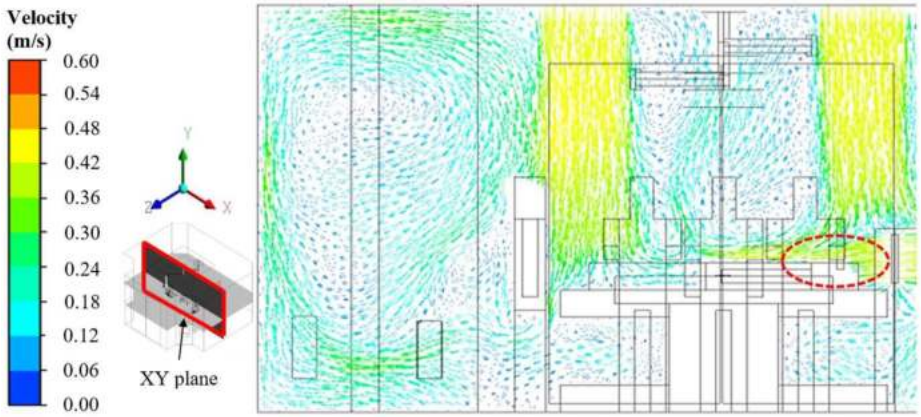

(d)

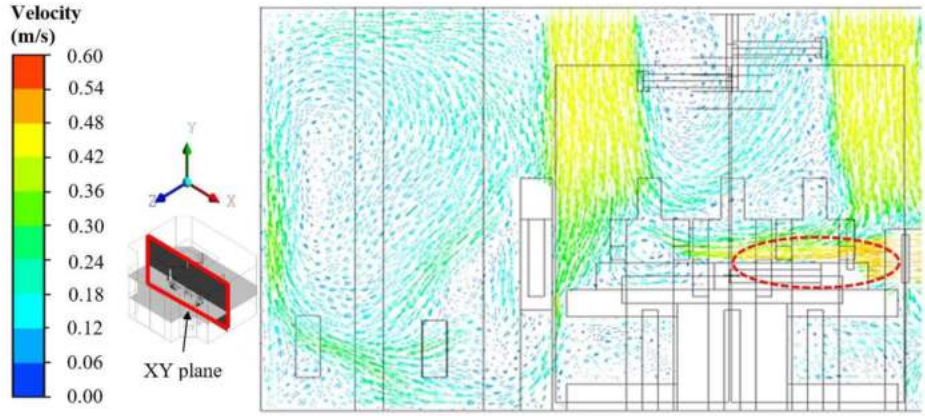

(e)

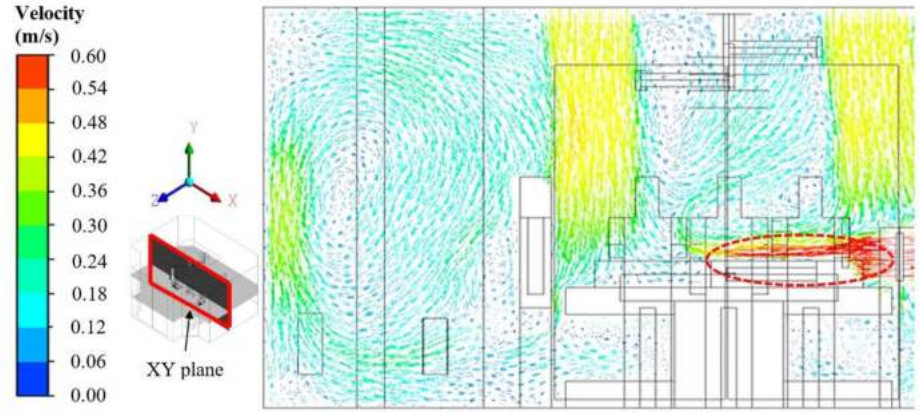

(f)

Fig. 14. (*continued*).

the air diffuser of the MAS unit. These vortices subsequently transport the infectious particles from the periphery into the surgical site [48]. The present study shows that an air velocity of 0.5 m/s provided the maximum wiping effect towards the dispersed particle in the surgical zone. This study outcome achieved a good consensus with the findings of Sadrizadeh and Holmberg [37], Sadrizadeh, Holmberg and Nielsen [47], Sadrizadeh, Tammelin, Nielsen and Holmberg [48], Sadrizadeh, Afshari, Karimipanah, Håkansson and Nielsen [55], where the air velocity of 0.4 m/s supplied from the MAS unit managed to flush the particle concentration above patient's region. Based on the present finding, the air velocity of 0.5 m/s was found to provide a maximum sweeping effect on the particles. Although the use of the MAS unit could not completely remove the particle concentration under the operating table, its concentration was reduced significantly compared to the condition without the activation of the MAS unit. The present study showed that the MAS unit only reduced the infectious particles within the airflow coverage

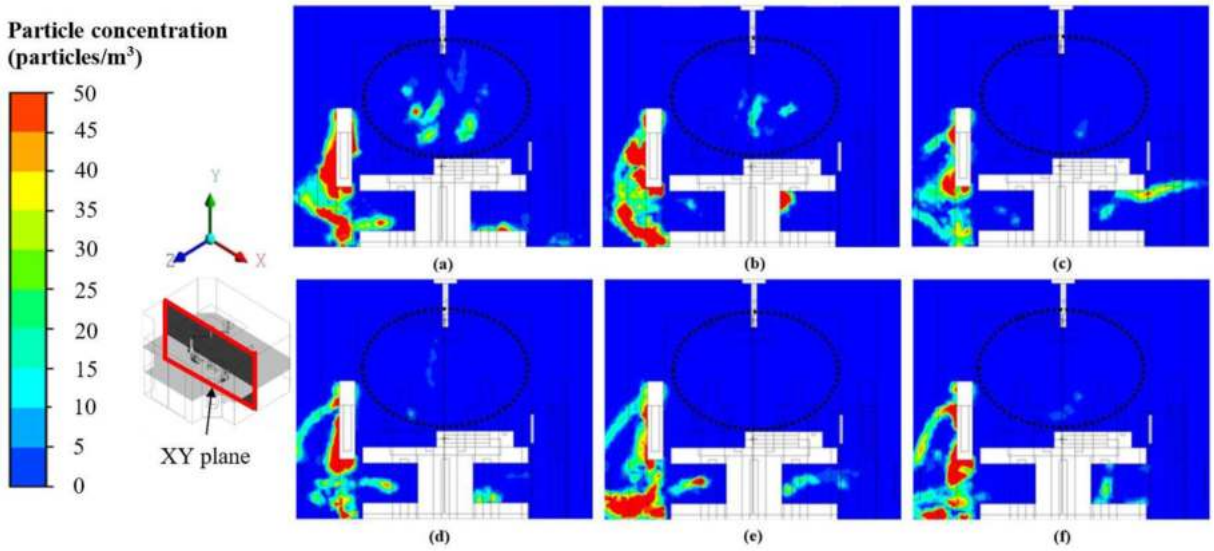

Fig. 15. Contour of particle concentration on XY plane that cut through the coordinate of z = 2.75 m when the MAS unit supplied air at velocity of (a) 0.1 m/s, (b) 0.2 m/s, (c) 0.3 m/s, (d) 0.4 m/s, (e) 0.5 m/s, and (f) 0.6 m/s.

region. Despite the presence of several medical staff members in the OR, a contaminant-free region in the surgical zone could be maintained with the use of the MAS unit.

4. Conclusions

The effectiveness of the MAS unit in reducing the concentration of the infectious particles above the region of the patient was examined under different supplied-air velocities. An RNG k-epsilon turbulent model was used to simulate the airflow in the operating room, while a DPM model based on the Lagrangian approach was used to track the particle dispersion. The CFD model was validated based on the good agreement (relative error <10%) between the simulated result and measured data published in the literature. The present study revealed the airflow distribution in the vicinity of the surgical site was relatively low, with an average velocity of approximately 0.11 m/s under the current ventilation system. The unidirectional airflow was quickly interrupted by the surgical lamp's fixture and the surgical lamps, thus hampering the effective removal of the airborne particles. Results showed that the activation of the MAS unit successfully reduced the airborne particle settlement by 78%, from approximately 45 particles/m^3 to 10 particles/m^3. When the MAS unit operates from 0.1 m/s up to 0.5 m/s, the particle concentration above the patient reduced gradually from 40 particles/m^3 to approximately 0 particles/m^3 while the clean region with the coverage distance increased from 0.242 m to 1.161 m. However, increasing the supplied air velocity to 0.6 m/s had an adverse effect on the particle concentration above the patient. Approximately 7 particles/m^3 were identified above the patient's region, although the airflow coverage could reach a maximum distance of 1.232 m. Therefore, this study suggested that the MAS unit shall be operated with 0.5 m/s to enhance the particle wiping efficiency during a surgical procedure. This recommended practice could lower the tendency of particle settlement on a patient's wound and subsequently reduce the risk of the patient contracting surgical site infection. Though a lower number of particles settled on the patient's wound could be expected, the efficiency of the MAS unit in reducing the contraction of SSI remained one of the limitations of current work. In a neuro- or more complex surgery that requires more surgical equipment and tools, the optimal placement of a MAS unit demands intensive investigation. Similarly, the suitable elevation angle and dimension of the air supply diffuser of the MAS unit could be an extended work to explore.

Authors' contribution

Conceptualization, methodology, funding acquisition, and writing of original draft: KYW; Conceptualization, methodology, and writing of original draft: HT, RAW, MHDO, BBN, GK; Methodology, editing, and reviewing: WYT, HYK, HSK, GRM; Reviewing and editing: DDVSC, WSH.

Funding

The authors would like to acknowledge Universiti Teknologi Malaysia through UTM Zamalah Grant (Vot. No. 00N04) provided for this study. This research was also funded by the Mini Research Grant by the Institution of Mechanical Engineers (IMechE), Malaysia Branch, under the Vot No. Of 4C587.

CRediT authorship contribution statement

Huiyi Tan: Writing – original draft, Methodology, Conceptualization. **Keng Yinn Wong:** Writing – original draft, Methodology, Funding acquisition, Conceptualization. **Mohd Hafiz Dzarfan Othman:** Writing – original draft, Methodology, Conceptualization. **Hong Yee Kek:** Writing – review & editing, Methodology. **Wah Yen Tey:** Writing – review & editing, Methodology. **Bemgba Bevan Nyakuma:** Writing – review & editing, Methodology, Conceptualization. **Guo Ren Mong:** Writing – review & editing, Methodology. **Garry Kuan:** Writing – original draft, Methodology, Conceptualization. **Wai Shin Ho:** Writing – review & editing. **Hooi Siang Kang:** Writing – review & editing, Methodology. **Desmond Daniel Chin Vui Sheng:** Writing – review & editing. **Roswanira Abdul Wahab:** Writing – original draft, Methodology, Conceptualization.

Declaration of competing interest

The authors declare that they have no known competing financial interests or personal relationships that could have appeared to influence the work reported in this paper.

Data availability

No data was used for the research described in the article.

Acknowledgement

The authors are grateful to Ir. Ts. Muhd Suhaimi Deris and engineers from Bumimaju MTE Engineering Sdn. Bhd. For providing consultation service to facilitate this study. Likewise, the authors would like to acknowledge Syahmi Bazlisyam Mohd Saupifor for extracting the simulation data.

References

[1] P. Uścinowicz, M. Chludzińska, A. Bogdan, Thermal environment conditions in Polish operating rooms, Build. Environ. 94 (2015) 296–304.
[2] J. Khodakarami, N. Nasrollahi, Thermal comfort in hospitals – a literature review, Renew. Sustain. Energy Rev. 16 (6) (2012) 4071–4077.
[3] M.G. Pizon, R.R. Baldo, R.N. Villarante, J.D. Balatero, Path Analysis of Covid-19 with the Influence of Air Pressure, Air Temperature, and Relative Humidity, Int. J. Adv. Res. (2021).
[4] H.M. Kamar, N. Kamsah, K.Y. Wong, M.N. Musa, M.S. Deris, Field measurement of airborne particulate matters concentration in a hospital's operating room, Jurnal Teknologi (Science & Engineering) 77 (30) (2015) 63–67.
[5] A.o.S. Technologists, Guidelines for Best Practices for Humidity in the Operating Room, 2017.
[6] T.J.H.i. McAuley, Specifications for temperature and humidity in sterile storage environments–Where's the evidence? Healthcare infection 14 (4) (2009) 131–137.
[7] M. Kohani, M. Pecht, New minimum relative humidity requirements are expected to lead to more medical device failures, Journal of Medical Systems 40 (3) (2016) 1–6.
[8] H. Tan, K.Y. Wong, B.B. Nyakuma, H.M. Kamar, W.T. Chong, S.L. Wong, H.S.J.E. S. Kang, P. Research, Systematic study on the relationship between particulate matter and microbial counts in hospital operating rooms, Environ Sci Pollut Res Int. 29 (5) (2022) 6710–6721.
[9] E. Najjar, A. Hallberg Kristensen, T. Thorvaldsen, M. Dalen, U.P. Jorde, L.H. Lund, Electrostatic discharge causing pump shutdown in HeartMate 3, JACC Case Rep 3 (3) (2021) 459–463.
[10] M. Kohani, M. Pecht, Malfunctions of medical devices due to electrostatic occurrences big data analysis of 10 Years of the FDA's reports, IEEE Access 6 (2018) 5805–5811.
[11] G. Caggiano, C. Napoli, C. Coretti, G. Lovero, G. Scarafile, O. De Giglio, M. T. Montagna, Mold contamination in a controlled hospital environment: a 3-year surveillance in southern, Italy 14 (1) (2014) 1–5.
[12] V. Kumar, S. Kumar, H. Kansal, Instrumentation Electronics, C. Engineering, Fuzzy logic controller based operating room air condition control system, Int. J. Appl. Innovat. Res. Electron. Electr. Eng. 2 (1) (2014) 510–514.
[13] R.P. Wenzel, Minimizing surgical-site infections, N. Engl. J. Med. 362 (1) (2010) 75–77.
[14] M. Loomans, W. Van Houdt, A. Lemaire, J.J.I. Hensen, B. Environment, Performance assessment of an operating theatre design using CFD simulation and tracer gas measurements 17 (4) (2008) 299–312.
[15] T. Chow, A. Kwan, Z. Lin, W. Bai, Conversion of operating theatre from positive to negative pressure environment, J. Hosp. Infect. 64 (4) (2006) 371–378.
[16] L.F. Shaw, I.H. Chen, C.S. Chen, H.H. Wu, L.S. Lai, Y.Y. Chen, F.J.B.i.d. Der Wang, Factors influencing microbial colonies in the air of operating rooms 18 (1) (2018) 1–8.
[17] T.D. Lindquist, T.D. Miller, J.L. Elsen, P.J.J.C. Lignoski, Minimizing the risk of disease transmission during corneal tissue processing, Cornea 28 (5) (2009) 481–484.
[18] A.J. Mangram, T.C. Horan, M.L. Pearson, L.C. Silver, W.R. Jarvis, H.I.C.P.A.C.J.I. Control, H. Epidemiology, Guideline for prevention of surgical site infection 20 (4) (1999) 247–280, 1999.
[19] S. Jain, M.J.S.I. Reed, Laminar air flow handling systems in the operating room 20 (2) (2019) 151–158.
[20] G. Birgand, C. Azevedo, S. Rukly, R. Pissard-Gibollet, G. Toupet, J.-F. Timsit, J.-C. Lucet, A.S.G.J.I. Control, H. Epidemiology, Motion-capture system to assess intraoperative staff movements and door openings, Impact on surrogates of the infectious risk in surgery 40 (5) (2019) 566–573.
[21] S. Sadrizadeh, A. Aganovic, A. Bogdan, C. Wang, A. Afshari, A. Hartmann, C. Croitoru, A. Khan, M. Kriegel, M. Lind, A systematic review of operating room ventilation 40 (2021), 102693.
[22] C.A. Balaras, E. Dascalaki, A.J.E. Gaglia, Buildings, HVAC and indoor thermal conditions in hospital operating rooms 39 (4) (2007) 454–470.
[23] T.C. Gormley, Assessment of the Environmental and Economic Impact of Air Changes in a Hospital Operating Room, 2016.
[24] A.A.o.A.f. Health, F.G. Institute, Guidelines for Design and Construction of Hospital and Health Care Facilities, Aia Press2001.
[25] N.L. Belkin, Use of scrubs and related apparel in health care facilities, Am. J. Infect. Control 25 (5) (1997) 401–404.
[26] P. Velusamy, K. Kiruba, K.N. Rajnish, T. Madhavan, P. Anbu, Recent Advances in the Development of Antimicrobial Nanotextiles for Prevention of Infectious Diseases Transmission in Healthcare Workers, 2021, pp. 17–26.
[27] W.C. White, R. Bellfield, J. Ellis, I.P. Vandendaele, Controlling the Spread of Infections in Hospital Wards by the Use of Antimicrobials on Medical Textiles and Surfaces, Medical and Healthcare textiles, Elsevier2010, pp. 55-75.
[28] A. Agirman, Y.E. Cetin, M. Avci, O. Aydin, Effect of laminar airflow unit diffuser size on pathogen particle distribution in an operating room, Science and Technology for the Built Environment 27 (4) (2020) 402–413.
[29] M.L. Ling, A. Apisarnthanarak, A. Abbas, K. Morikane, K.Y. Lee, A. Warrier, K. Yamada, APSIC guidelines for the prevention of surgical site infections, Antimicrob. Resist. Infect. Control 8 (2019) 174.
[30] L. Ridderstolpe, H. Gill, H. Granfeldt, H. Åhlfeldt, H. Rutberg, Superficial and deep sternal wound complications: incidence risk factors and mortality, Eur. J. Cardiothorac. Surg. 20 (6) (2001) 1168–1175.
[31] K.B. Kirkland, J.P. Briggs, S.L. Trivette, W.E. Wilkinson, D.J.J.I.C. Sexton, H. Epidemiology, The impact of surgical-site infections in the 1990s: attributable mortality, excess length of hospitalization, and extra costs 20 (11) (1999) 725–730.
[32] H. Tan, K.Y. Wong, C.T. Lee, S.L. Wong, B.B. Nyakuma, R.A. Wahab, K.Q. Lee, M. C. Chiong, W.S. Ho, M.H.D. Othman, H.Y. Kek, Y.H. Yau, H.M. Kamar, Numerical assessment of ceiling-mounted air curtain on the particle distribution in surgical zone, Journal of Thermal Analysis and Calorimetry (2022).
[33] A.C. von Vogelsang, P. Förander, M. Arvidsson, P. Löwenhielm, Effect of mobile laminar airflow units on airborne bacterial contamination during neurosurgical procedures, J. Hosp. Infect. 99 (3) (2018) 271–278.
[34] S. Barnes, C. Twomey, R. Carrico, C. Murphy, K. Warye, OR air quality: is it time to consider adjunctive air cleaning technology? AORN J. 108 (5) (2018) 503–515, 1.3, www.aornjournal.org/content/cme.
[35] J. Gamblin, J.M. Jefferies, S. Harris, N. Ahmad, P. Marsh, S.N. Faust, S. Fraser, M. Moore, P. Roderick, I. Blair, Nasal self-swabbing for estimating the prevalence of Staphylococcus aureus in the community, J. Med. Microbiol. 62 (3) (2013) 437–440.
[36] S.C. Mellinghoff, J.J. Vehreschild, B.J. Liss, O.A. Cornely, Epidemiology of surgical site infections with Staphylococcus aureus in europe: protocol for a retrospective, multicenter study, JMIR Res Protoc 7 (3) (2018) e63.
[37] S. Sadrizadeh, S. Holmberg, Effect of a portable ultra-clean exponential airflow unit on the particle distribution in an operating room, Particuology 18 (2015) 170–178.
[38] E. Goldman, L.H. Green, Practical Handbook of Microbiology, CRC press2015.
[39] U.P. Hebeisen, A. Atkinson, J. Marschall, N.J.A.R. Buetti, I. Control, Catheter-related bloodstream infections with coagulase-negative staphylococci: are antibiotics necessary if the catheter is removed? Antimicrob. Resist. Infect. Control 8 (1) (2019) 1–8.
[40] M. Chand, T. Lamagni, K. Kranzer, J. Hedge, G. Moore, S. Parks, S. Collins, C. del Ojo Elias, N. Ahmed, T.J.C.I.D. Brown, Insidious risk of severe Mycobacterium chimaera infection in cardiac surgery patients 64 (3) (2017) 335–342.
[41] T. Hamza, M. Dietz, D. Pham, N. Clovis, S. Danley, B.J.E.c. Li, materials, Intra-cellular Staphylococcus aureus alone causes infection in vivo 25 (2013) 341.
[42] G. Cao, A.M. Nilssen, Z. Cheng, L.I. Stenstad, A. Radtke, J.G. Skogas, Laminar airflow and mixing ventilation: which is better for operating room airflow distribution near an orthopedic surgical patient? Am. J. Infect. Control 47 (7) (2019) 737–743.
[43] S. Fischer, M. Thieves, T. Hirsch, K.D. Fischer, H. Hubert, S. Beppler, H.M. Seipp, Reduction of airborne bacterial burden in the OR by installation of unidirectional displacement airflow (UDF) systems, Med. Sci. Mon. Int. Med. J. Exp. Clin. Res. 21 (2015) 2367–2374.
[44] T. Hirsch, H. Hubert, S. Fischer, A. Lahmer, M. Lehnhardt, H.U. Steinau, L. Steinstraesser, H.M. Seipp, Bacterial burden in the operating room: impact of airflow systems, Am. J. Infect. Control 40 (7) (2012) e228–e232.
[45] D. Casagrande, M. Piller, Conflicting Effects of a Portable Ultra-clean Airflow Unit on the Sterility of Operating Rooms: A Numerical Investigation, Build. Environ. vol. 171 (2020).
[46] R. Lapid-Gortzak, R. Traversari, J.W. van der Linden, S.Y. Lesnik Oberstein, O. Lapid, R.O. Schlingemann, Mobile ultra-clean unidirectional airflow screen reduces air contamination in a simulated setting for intra-vitreal injection, Int. Ophthalmol. 37 (1) (2017) 131–137.
[47] S. Sadrizadeh, S. Holmberg, P.V. Nielsen, Three distinct surgical clothing systems in a turbulent mixing operating room equipped with mobile ultraclean laminar airflow screen: a numerical evaluation, Science and Technology for the Built Environment 22 (3) (2015) 337–345.
[48] S. Sadrizadeh, A. Tammelin, P. Nielsen, S. Holmberg, Does a mobile laminar airflow screen reduce bacterial contamination in the operating room? A numerical study using computational fluid dynamics technique, Patient Saf. Surg. 8 (2014) 27.
[49] C. Pasquarella, G.E. Sansebastiano, S. Ferretti, E. Saccani, M. Fanti, U. Moscato, G. Giannetti, S. Fornia, P. Cortellini, P. Vitali, C. Signorelli, A mobile laminar airflow unit to reduce air bacterial contamination at surgical area in a conventionally ventilated operating theatre, J. Hosp. Infect. 66 (4) (2007) 313–319.
[50] S. Friberg, B. Ardnor, R. Lundholm, B. Friberg, The addition of a mobile ultra-clean exponential laminar airflow screen to conventional operating room ventilation reduces bacterial contamination to operating box levels, J. Hosp. Infect. 55 (2) (2003) 92–97.
[51] S.I. Tanabe, L. Tacutu, I. Nastase, F. Bode, A. Dogeanu, C. Croitoru, H. Zhang, J. Kurnitski, M.C. Gameiro da Silva, I. Nastase, P. Wargocki, G. Cao, L. Mazzarela, C. Inard, Local and general ventilation system for an operating room with surgeons and patient, E3S Web of Conferences 111 (2019).
[52] M. Thore, L.G. Burman, Further bacteriological evaluation of the TOUL mobile system delivering ultra-clean air over surgical patients and instruments, J. Hosp. Infect. 63 (2) (2006) 185–192.

[53] B. Friberg, M. Lindgren, C. Karlsson, A. Bergstrom, S. Friberg, Mobile zoned/exponential LAF screen: a new concept in ultra-clean air technology for additional operating room ventilation, J. Hosp. Infect. 50 (4) (2002) 286–292.
[54] P.M. Bluyssen, M. Ortiz, D. Zhang, The effect of a mobile HEPA filter system on 'infectious' aerosols, sound and air velocity in the SenseLab, Build. Environ. 188 (2021), 107475.
[55] S. Sadrizadeh, A. Afshari, T. Karimipanah, U. Håkansson, P.V. Nielsen, Numerical simulation of the impact of surgeon posture on airborne particle distribution in a turbulent mixing operating theatre, Build. Environ. 110 (2016) 140–147.
[56] C. Wang, S. Holmberg, S. Sadrizadeh, Numerical study of temperature-controlled airflow in comparison with turbulent mixing and laminar airflow for operating room ventilation, Build. Environ. 144 (2018) 45–56.
[57] H.M. Kamar, K.Y. Wong, N. Kamsah, The effects of medical staff turning movements on airflow distribution and particle concentration in an operating room, Journal of Building Performance Simulation 13 (6) (2020) 684–706.
[58] K. Wong, H. Kamar, N. Kamsah, Medical staff's posture on airflow distribution and particle concentration in an operating room, in: IOP Conference Series: Materials Science and Engineering, IOP Publishing, 2020, 012103.
[59] K.Y. Wong, H. Tan, B.B. Nyakuma, H.M. Kamar, W.Y. Tey, H. Hashim, M. C. Chiong, S.L. Wong, R.A. Wahab, G.R. Mong, W.S. Ho, M.H.D. Othman, G. Kuan, Effects of Medical Staff's Turning Movement on Dispersion of Airborne Particles under Large Air Supply Diffuser during Operative Surgeries, Environmental Science and Pollution Research, 2022.
[60] M. Bern, P. Plassmann, Mesh Generation, Handbook of Computational Geometry, 2000.
[61] M.S. Mat Ali, C. Doolan, V. Wheatley, GRID CONVERGENCE STUDY for A TWO-DIMENSIONAL SIMULATION of FLOW AROUND A SQUARE CYLINDER at A LOW REYNOLDS NUMBER, Seventh International Conference on CFD in the Minerals and Process Industries, CSIRO, Melbourne, Australia, 2009, pp. 1–6.
[62] B. Zhao, C. Yang, C. Chen, C. Feng, X. Yang, L. Sun, W. Gong, L. Yu, How many airborne particles emitted from a nurse will reach the breathing zone/body surface of the patient in ISO class-5 single-bed hospital protective environments?—a numerical analysis, Aerosol. Sci. Technol. 43 (10) (2009) 990–1005.
[63] X. Ho, W.S. Ho, K.Y. Wong, M.H. Hassim, H. Hashim, Z. Ab Muis, N.A. Yunus, G.H. T. Ling, Study of fresh air supply vent on indoor airflow and energy consumption in an enclosed space, Chem. Eng. 83 (2021).
[64] S. Paudel, N. Saenger, Grid refinement study for three dimensional CFD model involving incompressible free surface flow and rotating object, Comput. Fluids 143 (2017) 134–140.
[65] J. Liu, H. Wang, W. Wen, Numerical simulation on a horizontal airflow for airborne particles control in hospital operating room, Build. Environ. 44 (11) (2009) 2284–2289.
[66] D. Hansen, C. Krabs, D. Benner, A. Brauksiepe, W. Popp, Laminar air flow provides high air quality in the operating field even during real operating conditions, but personal protection seems to be necessary in operations with tissue combustion, Int. J. Hyg Environ. Health 208 (6) (2005) 455–460.
[67] L. Tacutu, I. Nastase, F. Bode, A. Dogeanu, C. Croitoru, Ieee, Interaction between a Local and a General Ventilation System for an Operating Room with Patient, in: INTERNATIONAL CONFERENCE ON ENERGY AND ENVIRONMENT, CIEM, 2019, pp. 348–353, 2019.
[68] S. Sadrizadeh, S. Holmberg, P.V. Nielsen, Three distinct surgical clothing systems in a turbulent mixing operating room equipped with mobile ultraclean laminar airflow screen: a numerical evaluation, Science and Technology for the Built Environment 22 (3) (2016) 337–345.
[69] S. Sadrizadeh, S. Holmberg, Effect of a portable ultra-clean exponential airflow unit on the particle distribution in an operatng room, Particuology 18 (2015) 170–178.
[71] Z. Zhang, W. Zhang, Z.J. Zhai, Q.Y. Chen, Evaluation of various turbulence models in predicting airflow and turbulence in enclosed environments by CFD: Part 2—comparison with experimental data from literature, HVAC R Res. 13 (6) (2007) 871–886.
[72] K.Y. Wong, M.K. Haslinda, K. Nazri, S.N. Alia, Effects of surgical staff turning motion on airflow distribution inside a hospital operating room, Evergreen 6 (1) (2019) 52–58.
[73] K. Wong, H. Kamar, N. Kamsah, Enhancement of airborne particles removal in a hospital operating room, Int. J. Automot. Mech. Eng. 16 (4) (2019) 7447–7463.
[74] N. Kamsah, H.M. Kamar, M.I. Alhamid, K.Y. Wong, Impacts of temperature on airborne particles in a hospital operating room, Journal of Advanced Research in Fluid Mechanics and Thermal Sciences 44 (1) (2018) 12–23.
[75] C. Yang, X. Yang, T. Xu, L. Sun, W. Gong, Optimization of Bathroom Ventilation Design for an ISO Class 5 Clean Ward, Building Simulation, Springer, 2009, pp. 133–142.
[76] G. Cao, M.C.A. Storas, A. Aganovic, L.I. Stenstad, J.G. Skogas, Do surgeons and surgical facilities disturb the clean air distribution close to a surgical patient in an orthopedic operating room with laminar airflow? Am. J. Infect. Control 46 (10) (2018) 1115–1122.
[77] A.S.H.R.A.E. Guidelines, HVAC Design Manual for Hospitals and Clinics, ASHRAE Inc, 2003.
[78] A. Emil, K.B. Lital, A. Eithan, M. Tamar, R. Alia, N. Faris, Surgical site infections after abdominal surgery: incidence and risk factors. A prospective cohort study, INFECTIOUS DISEASES 47 (11) (2015) 761–767.
[79] S. Ceken, S.S. Yavuz, A. Sensoy, O. Imamoglu, Epidemiology and risk factors for surgical site infections following thoracic surgery, Int. J. Clin. Exp. Med. 9 (6) (2016) 12018–12024.